THE RESPONSE TO SHIP MOTIONS OF TOWED VEHICLES

FOR USE AS OCEANIC MICROSTRUCTURE MEASUREMENT PLATFORMS

BY
GUY A. SANTORA

Thesis submitted to the Faculty of the Virginia Polytechnic Institute and State University in partial fulfillment of the requirement for the degree of

MASTER OF SCIENCE

IN

AEROSPACE AND OCEAN ENGINEERING

APPROVED:

P. KAPLAN, CHAIRMAN

J. A. SCHETZ

W. NEU

DECEMBER, 1985

BLACKSBURG, VIRGINIA

THE RESPONSE TO SHIP MOTIONS OF TOWED VEHICLES

FOR USE AS OCEANIC MICROSTRUCTURE MEASUREMENT PLATFORMS

BY
GUY A. SANTORA

Committee Chairman: Paul Kaplan
Aerospace and Ocean Engineering

(ABSTRACT)

The response to ship induced motions has been predicted for four towed underwater vehicles. The purpose of the study is to determine the suitability of these vehicles for their use as oceanic microstructure sensor carrying platforms. All have been used in the past for oceanic studies, and these four vehicles show the most promise for microstructure work.

Transfer functions which describe the response of a towed vehicle have been determined, for longitudinal motions. Also, the motion spectra of the vehicles have been predicted for the longitudinal mode as a result of being towed by a typical research vessel in a sea state three.

TABLE OF CONTENTS

LIST OF FIGURES

LIST OF FIGURES

(Continued)

LIST OF FIGURES

(Continued)

LIST OF FIGURES

(Continued)

LIST OF TABLES

INTRODUCTION

In recent years the study of small scale structures of the physical parameters within the ocean have lead to a vastly increased understanding of these structures. However, data of this type is somewhat scarce, especially at the microstructure scale. Parametric quanification within one and one half feet may be considered as microstructure. The problem lies with being able to deploy a stable sensor platform within the ocean. By far, the most difficult parameter to measure is turbulent oceanic velocities, where velocities of interest may be less than 0.1 ft/sec. The ability to measure such small perturbations of physical parameters depend on such factors as frequency response and spatial resolution of the sensors themselves. It is these factors, which to a large extent, dictate how stable the platform must be.

There are several methods of obtaining microstructure data, such as, moored, expendable, tethered, free-swimming and towed systems. Because of the desire to obtain data over large areas of the oceans, the use of moored or expendable devices is not feasible. Tethered systems as well as free-swimming submersibles are typically relatively slow. In addition, free-swimming systems are required to contain data acquisition and data storage equipment, also they tend to be very expensive to design, manufacture, and operate. Because of these considerations the towed system is most attractive.

In order to provide accurate and consistent oceanic microstructure data, a system is required which will unify the wide variety of those sensors which are currently being utilized on different platforms. Several agencies have been gathering this information with some success for several years. The

problem lies with consolidating the data gathered using sensors having different limitations and noise characteristics as well as different platform motion characteristics.

An effort has been undertaken to successfully gather microstructure data as well as coordinate the data collection and to ease the task of data comparison.

This effort consists of definition of sensor, telemetry and vehicle requirements. The present study examines the vehicle requirements and vehicle motions in an attempt to aid this effort.

Four towed vehicles currently being used for oceanographic work have been examined to determine their suitability for oceanic microstructure measurements namely; their response to tow ship motions.

In each case, response motion spectra of each vehicle have been computed. Then, the significant motion amplitudes within the frequency range of interest were used for comparison. The vehicle motions were compared in part to each other and in part against motion limits where they were specified.

TOWED VEHICLE REQUIREMENTS

Listed below are basic vehicle requirements, along with an explanation of the impact to the mission if these requirements are not met.

- Depth Range: 30 - 1500 feet

without this specified depth range capability the system will be limited in vertical coverage at some (or all) speeds of interest.

- Speed Range: 2 - 12 knots

If the maximum speed of 12 knots is not obtained, a longer amount of time is required to gather an equivalent amount of data. This is unlikely to severely impact the mission, unless the speed reduction is excessive. However, the two knot minimum is a strict requirement as this is approximately the minimum maneuvering speed for typical research vessels.

- Sufficient Payload Capacity: (In both weight and volume) to carry necessary instrumentation.

It goes without saying that the body must be able to carry the required sensors and support electronics. For information regarding the physical, electrical and data requirements for the vehicle, the reader is referred to a report by Santora.[1]

[1]Santora, G. A. and Crane, J., (1985), "Sensor Requirements for Fine-Scale Ocean Microstructure Vehicles," NCSC, Tech. Memo JAN 1985.

- Depth Control: Ability to maintain depth, oscillate, or follow an isometric contour within +/- 1.5 feet. .[2]

Without the ability to maintain a desired depth, data may become contaminated by vertical structures of various parameters. This may or may not be critical as long as vehicle depth is known. Instead of maintaining a constant depth, many researchers prefer to slowly oscillate in depth. Typical oscillation are on the order of several feet in amplitude, with a period on the order of one minute.

- Body Motions/Vibrations: Low enough that resulting sensor motion effects may be neglected or compensated for.

Uncontrolled body motions and vibrations are the biggest problem in microstructure sensing from a towed vehicle. Primarily it is the velocity sensors that are affected. Although different velocimeters are affected differently by the various pertubations of the body, the problem lies with differentiating between turbulent velocities and velocities of the body (sensor). While accelerometers may be placed in close proximity of the sensors to measure sensor movement, the removal of sensor motion from the data remains a controversial issue. In short, a tow platform is required which undergoes minimal pertubations from its desired position.

[2]Koeppen, S.H. (1979), "A Study of the Use of A Towed Body for Ocean Fine and Microstructure Measurements," MAR Tech. Rept. No. 226.

MOTION COMPENSATION

The addition of a ship borne motion compensation system to the towed system hardware can significantly improve overall performance in terms of ship motion decoupling. There are several types of motion compensation systems, however all attempt to maintain a constant tension at the ships tow point. Two of the most common types of systems are actively controlled and are described briefly here.

The motion compensation winch appropriately pays out and reels in cable when tow cable tensions raise and fall, respectfully. This type of system is often slow to respond in commonly encountered short period waves.

The constant tension arm (or piston) is attached directly to the tow cable sheave. This sytem raises and lowers the effective ships tow point in an attempt to hold the tension constant. Due to the relatively low inertia of these systems, they are capable of responding much faster than the active winch system.

Unfortunately, reliable data on the effectiveness of motion compensation systems is rare. However, Dugan[3] of NRL has conducted a study of such a device.

Dugan utilized a Western Gear guidelines tensioner (model no. D306140) acting as a hydraulic piston. Figure 1 presents the transfer function of the tensioner which was estimated from motion spectrum data of tow body depth taken with and without the tensioner active. The figure shows that it is possible to achieve motion reduction in the frequency band of 0.01

to 1 hertz with a maximum reduction of nearly two orders-of-magnitude at 0.1 hertz (.628 rad/s).

GENERAL DISCUSSION OF TOWED BODIES FOR USE IN MICROSTRUCTURE MEASUREMENTS

Towed underwater vehicles have been designed and successfully flown within the speed and depth ranges of interest to microstrucrture study. Also, there are vehicles which have acceptable levels of body motions. The problem lies with obtaining all these requirements.

Ship coupled vehicle motions are occassionally measured, also, they are predictable (as in this study). Unfortunately vehicle vibrations are rarely measured and extremely difficult to predict. However, we do have a reasonably good understanding of the mechanics involved.

VEHICLE VIBRATIONS

Although the primary purpose of the present study is to predict the tow ship induced motions of several existing towed bodies, motions due to vibrations of the tow cable, and of the body itself are important when considering a towed body for use as a microstructure sensor platform. This section is intended to help the reader gain some insight to the problem of towed vehicle vibrations.

Vehicle vibrations can be attributed to the two major sources, self noise of the body itself and cable strumming. What is meant by the term self noise is the vibrations induced by the body moving through a viscous fluid. Two major sources of self noise are vortex shedding, and pressure fluctuations due to turbulent boundary layers.

The shedding of vortices occurs when, at high Reynolds numbers, the flow behind a body is no longer streamline. Separation of the flow occurs, and vortices are formed. The strength of the vortices increases with the Reynolds number. A high frequency pressure fluctuation and vibration of the body is the result. If vortex shedding occurs on a fin or appendage, the vibrations are amplified by the bending and torsional modes of the fin. The frequency of shedding (and vibrations) are governed by the size of the body and the velocity (Strouhal number). Vortice shedding may be reduced by a streamlined body with small pitch and yaw angles.

Turbulent boundary layers cause body vibrations in a similar manner as does vortex shedding. In fact within the turbulent layer are small scale vortices called turbulent eddies which cause an unsteady pressure distribution along the body. This fluctuating pressure causes the body to vibrate. Turbulent eddies may be reduced with a streamlined body.

As velocity is increased, the higher frequencies of the motion spectrum (vibrations) are amplified while the lower frequencies attenuated slightly.

Cable strumming is probably the major source of vehicle vibration. Strumming is due to the periodic alternately shed vortices around the sides of the cable. This may occur at any angle of attack, but the phenomenon increases as angle of attack increases and is maximum when the cable is perpendicular to the flow, Figure 2. This periodic shedding of vortices excite the system into resonant vibrations if the frequency of shedding is close to one of the natural frequencies of the system. The cable is free to vibrate in any mode corresponding to multiples of its fundamental frequency and the

vortex forcing will sort out a harmonic that is sufficiently close to the shedding frequency and will produce resonance. Frequencies of flow induced cable strumming are in the region of 8 to 30 hertz, for typical towed systems.

Due to the very low damping associated with tow cables, large amplitude vibrations can occur. These large amplitude vibrations produce very broad band "lock-in" regions, as shown in Figure 3. The amplitude of the cable vibrations are only limited by the breakdown of the vortices at large amplitudes. Experiments indicate that maximum peak-to-peak displacement of typical tow cables is approximately 3.6 diameters.

In addition to causing towed vehicles to vibrate, cable strumming can significantly increase the drag of the cable, and hence, of the system. Bare armored tow cables have a drag coefficient of approximately 1.2 at Reynolds numbers of order 10^4. This drag coefficient has been seen to be as large as 2.0 during highly excited strumming.

Vehicle vibrations due to tow cable strumming may be minimized by maintaining a near horizontal cable catenary and by minimizing tensions at the vehicles tow point, as higher tensions allow more of the cable vibrations to be transmitted to the body. Unfortunately, both of these conditions preclude deep, fast tows.

Tow cable strumming may be significantly reduced by the additions of trailing ribbons, streamlined fairing or helical wrap. Trailing ribbons, in the wake of the cable, interfere with the formation of vortices. Streamlined fairings basically intercept the separation point of the boundary layer so that

adverse pressure gradients are minimized. By spiral wrapping a small diameter wire around the cable, the boundary layer is tripped at different span wise locations, thus disrupting the periodicity of the formation.

The drawbacks to these methods are, increase in the drag coefficient, increased difficulty in handling, or reduced durability.

PROCEDURE

The vehicle/cable systems were analyzed with the aid of the semi-empirical hydrodynamic analysis methods developed at NCSC. The Hydrodynamic Analysis Techniques (HYDAT) system of computer programs was dedveloped for the purpose of underwater vehicle design and analysis. The system consists of five modular analytic programs, each of which performs a specific function in predicting the performance, stability, and control of submersible vehicles.

A block diagram of HYDAT appears in Figure 4, the following is a brief discussion of the modules used in this study.

The first of the HYDAT modules used in this analysis is the HYGEOM module which accepts basic geometrical data, calculates geometrical quantities such as volume, surface area, centers of mass and bouyancy, and moments and products of inertia. All of these quantities may be overrided by the user. It then processes the data for further use as well as for plotting. A vehicle is modelled as a build up of a number of components such as, bodies, fins, control surfaces, decks, thruster, shrouds, pods and ballast tanks. Bodies may be of circular, elliptic, Lewis form or semi-arbitrary in cross setion. Fins and control surfaces are symmetric airfoils of the four digit NACA series. However, a control surface may be a fraction of the associated fin. Pods are small axisymmetric bodies.

The above components are those which are most commonly found on submersible vehicles. These components which compose the vehicle are

attached to each other in a specific manner. Each component is defined in a local coordinate system (LSC) relative to the general coordiante system (GCS) or another component. The module uses Euler angle transformations to orient a LCS with respect to the GCS. In this manner HYGEOM keeps track of which components are attached to each other and the interference effects may be calculated in a subsequent module.

In short, HYGEOM serves as an input for basic vehicle data as well as a visual checkout by plotting a three view drawing of the assembled components.

The HYCOEF module reads process data provided by HYGEOM, it then calculates the total vehicle hydrodynamic coefficients. These coefficients may be divided into three groups; body, fin/control surface, and propulsion. The latter will not be discussed here.

The body coefficients may be subdivided into linear and nonlinear coefficients. The linear coefficients include static, added mass and rotational coefficients, these are derived from slender body theory. The nonlinear coefficients include those which arise from viscous flow along the body, and second-order cross-coupling coefficients derived from potential flow theory.

The coefficients of fins and controls surfaces are primarily computed using standard formulas which have been made available from the Air Force. These methods are semi-empirical in nature and are the basis of many aircraft flight simulation computer programs. Included in these methods are

formulas for computing various interferences between the vehicle components.

Also in the late 1970's NCSC initiated a series of wind tunnel tests of a series of bodies and body/fin geoemtries. The purpose and result of these tests were to gather enough experimental data to develop semi-empirical methods for the prediction of linear coefficients of similar geometries.

In comparison with data in the literature, whether hydrodynamic coefficients or stability derivatives, HYCOEF does a remarkably good job of prediction.

The HYCABL module is used to calcuate the three-dimensional steady state, static, cable catenary by using the linear cable derivatives of a towed body/cable system. HYCABL may be used in conjunction with HYDAT or as a stand-alone program. When provided with the body hydrodynamic coefficients, HYCABLE also calculates the equilibrium body orientation. This is accomplished by simply solving for the three Euler angles (roll, pitch, yaw) in the vehicle equations of motion with all moments equal to zero.

HYCABL computes the system cable catenary by integrating the linear cable equations along the cable. The six linear equations are partial differentials of tension, the two cable angles, and the three spatial coordinates with respect to cable length. Initial conditions are the inertial tension components at the vehilcle end, which are obtained by solving the force equations of motion at the equilibrium orientation of vehicle. The cable equations are

then integrated from the tow body up the cable to the tow ship. An iteration of this integration is continued until a solution is found.

Cable properties are also required in solving for the catenary. Basic input are cable weight, diameter length and drag coefficients. These cable drag coefficients are in terms of loading functions which describe both normal and tangential drag as a function of cable angle (ϕ). The form for these loading functions are shown below, where ϕ is the cable angle measured from the vertical.

$$F_T = A_{TO} + A_{T1}\,COS(\phi) + B_{T1}\,SIN(\phi) + A_{T2}\,COS(2\phi) + B_{T2}\,SIN(2\phi)$$

and

$$F_N = A_{NO} + A_{N1}\,COS(\phi) + B_{N1}\,SIN(\phi) + A_{N2}\,COS(2\phi) + B_{N2}\,SIN(2\phi)$$

The coefficients, A's and B's, have been determined experimentally for typical tow cables by various investigators. Both F_T and F_N are multiplied by the normal drag coefficient to find the tangential and normal drag per unit cable length, respectfully.

After the cable equations have been integrated, a set of cable derivatives, relating tensions to displacements at the upper and lower tow points (similar to the spring constants of classical mechanics) is calculated. The output is presented in the form of a stiffness matrix. This is an extremely handy feature, especially for application to the present study, as will be seen.

The HYTFUN module performs linear system analysis of both free-swimming and towed vehicle systems. Basically, it uses the linearized

equations of motion to compute the eigenvalues and eigenvectors of the sytem. Also it computes transfer functions and frequency responses (Bode Plots).

The transfer functions computed are those relating changes in vehicle controls, such as control surfaces and thrusters, to vehicle states. Unfortunately, these transfer functions do not lend themselves to the present study. What is required here are transfer functions which related displacements of the upper towpoint to vehicle states.

In order to calculate these vehicle transfer functions the state and control matrices are required (Appendix A). These matrices are computed by HYTFUN and uncoupled into longitudinal and lateral sets. Also required is the disturbance (ship towpoint motion) matrix which contains the stiffness matrix produced by HYCABLE along with mass coefficients. Refering to Appendix A for notation, the equations are;

$$(1) \qquad \{\dot{X}\} = [A]\{X\} + [B]\{U\} + [D]\{V\}$$

or in the frequency domain, utilizing La Place transforms

$$(2) \qquad X_{(s)} = (sI - A)^{-1}[X_{(o)} + B\,U_{(s)} + DV_{(s)}]$$

Now it is convient to define the response vector as,

$$(3) \qquad \{C\} = [E]\{X\} + [F]\{U\} + [G]\{V\}$$

or again in the frequency domain

(4) $C_{(s)} = E\,X_{(s)} + F\,U_{(s)} + G\,V_{(s)}$

However, since we are conserned with the response of the vehicle state vector, equation 4 reduces to

(5) $C_{(s)} = E\,X_{(s)}$

Upon inserting equation 2 into 5, we obtain

(6) $C_{(s)} = E\,(sI - A)^{-1}\ (BV_{(s)} + DV_{(s)})$

Since the definition of a transfer function requires the initial conditions to be zero, the transfer function of interest (vehicle state to ship motion) is,

(7) $H_{(s)} = E\,(sI - A)^{-1}\,DV_{(s)}$

E is a matrix of primary zeros containing a unit vector in the column representing the particular state response in question. Sixth order polynomials are obtained for both longitudinal and lateral motions, which are of the form,

(8)

$$H_{(s)} = \left\{ \frac{N_1 S^5 + N_2 S^4 + N_3 S^3 + N_4 S^2 + N_5 S + N^6}{S^6 + D_1 S^5 + D_2 S^4 + D_3 S^3 + D_5 S + D_6} \right\}$$

Each of the four vehicle geometries in question are input into HYGEOM. In the case of one of the vehicle which employs a cambered wing section, the input was modified to account for the camber. Basically, the angle of attack

for zero lift was calcualted for the cambered wing. This value was input as an offset to the actual angle of attack.

A towed vehicles response to ship motions is a function of the cable catenary. Tensions at the vehicle and cable drag forces are what determine the shape of the catenary. Because of this, an attempt is made to position the vehicles at depth with minimum tension using cable scope (length) and control surfaces, where possible, while maintaining reasonably low values of pitch and control surface deflection.

Each of the vehicles have been analyzed at three speeds and four depths. These speeds are 2.5, 5.0 and 8.0 knots and correspond to tow ship speeds of available ship motions. Depth of 30, 500, 1000 and 1500 feet have been used for the analysis. The results have been verified, where possible, with documentation of the systems. Tow vehicle/cable system configurations appear in Tables 1 through 4.

Once system configruations and tow cable stiffness matrices are obtained, the systems are analyzed for stability and the state and control matrices are obtained through use of HYTFUN, for each vehicle, speed and depth.

Upon linearization of the state equations, positive roots appeared in the characteristic equations of vehicles B and D. These unstable eigenvalues are associated with the longitudinal state depth, which indicates both vehicles are unable to maintain depth without some type of control system. Vehicle B has associated with it a single real positive root, indicating an

expontial divergence from its steady state depth position. Vehicle D possessed a pair of complex roots with positive real parts, which indicate an oscillatory divergence in depth.

At this point in the study information concerning the actual control systems of these two vehicles was needed. Upon conversations with the vehicles users, these instabilities were verified. However, no documentation concerning the control system of vehicle B could be obtained without considerable effort. Vehicle D is flown with adjustable gains which are varied with vehicle speed, depth and cable scope. Again, no documentation could be made avilable. Essentially the only fact known concerning these two control systems is that both employ state feedbacks of pitch, pitch rate and depth.

As a result of the lack of knowledge of the control systems, for the purpose of this study, a state feedback control system has been modelled. An algorithm was written which solves for a feedback gain vector which will produce a stable system. The states employed are those of the actual systems, namely, pitch, pitch rate and depth. The algorithm employed an iterative Monte Carlo simulation scheme to find stable eigenvalues corresponding to the closed loop system matrix. The associated gains are required to produce a stable vehicle throughout the depth and speed regime of interest. No consideration was given to damping ratio, signal to noise ratio, etc. However, the magnitude of the gains are restricted to reasonable values. The new closed loop system is obtained by subtracting from the original state matrix the new gain matrix times the control matrix, as shown below.

(9) $$\{\dot{X}\} = [A]\{X\} + [B]\{U\} + [D]\{V\}$$

is the original dynamic equation. The closed loop system is formed by feeding back the state vector through a gain matrix G.

(10) $$\{U\} = -[G]\{X\}$$

so the closed loop system may be described by,

(11) $$\{\dot{X}\} = [[A] - [B][G]]\{X\} + [B]\{U\} + [D]\{V\}$$

Once a stable system is acquired and transfer functions have been obtained, through the procedure shown earlier, the ship motions are required to solve for vehicle response. Ship motions, in the form of motion spectra, have been obtained for the research vessel Cape Henlopen.[5] In that report ship motion spectra are obtained experimentally in a sea state 3, with significant wave heights ranging from 2.47 to 3.41 feet. Longitudinal motion spectra for heave and pitch were presented in the report. Unfortunately, ship transfer functions, which yield heave/pitch relations, were unavailable. Consequently, the assumption was made that heave of the tow point is that of the ship, however, the objective here is to compare motions of the towed vehicles and not to predict their actual motions in response to a specific towship in a specific sea way.

[5]Kallio, J. A. (1977), "Seakeeping Trials of the R/V Cape Henlopen", DTNSRDC, Rept. No. 77/041, July 1977

Towed vehicle motion response spectra are obtained by numerically multipling the magnitude of the transfer function squared by the ship motion specrtra at corresponding values of frequency. The range of frequencies is governed by the available range of the ship motion spectra. A particular transfer function is written as;

$$H_{(s)} = H_{(i\omega)}$$

(12) $$|H_{(\omega)}|^2 = H_{(i\omega)} H_{(-i\omega)}$$

then the response spectrum $S_R(\omega)$

(13) $$S_{R(\omega)} = |H_{(\omega)}|^2 S_{ship(\omega)}$$

Once the vehicle response spectrum is obtained, the significant motion is computed. This is accomplished by integrating the spectrum over the frequency. Two times the square root of this quantity is defined as the significant motion.

(14) $$X_{sig} = 2\sqrt{\int S_R(\omega)\, d\omega}$$

The performance of the candidate towed systems are measured in part against each other and against requirements presented by Dugan[6] of NRL. These requirements are presented as permissible significant motion amplitude (twice the R.M.S. value) as a function of frequency range in Figure 5.

[6]Dugan, J. P. and Morris, W. D. (1984), "Instrumentation Requirements for Small Scale Towed Temperature measurements," NRL Memo Rept. No. 5288

In obtaining towed vehicle significant motions, each towed vehicle motion spectrum has been integrated from 0.5 to 1.4 radians per second. This corresponds to the lowest frequency band (0.8 - 1.4 rad/sec) in Figure 5. The assumption was made that all motions corresponding to frequencies of less than 0.8 rad/sec are permissible, since no restrictions are given.

In order to compare the results obtained in this analysis with the permissible significant towed vehicle motions presented in Figure 5, some assumptions are required. First, since no vehicle motion phase information has been obtained, all significant motion magnitudes are superimposed to yield a total significant motion. Although this is a highly unlikely occurance, it does represent the worst possible case. Secondly, the sensors are assumed to be located at the nose of the vehicle. This enables one to readily decompose vehicle pitch into surge and heave of the sensor suite. This is also where most researchers prefer to place their sensors, enabling them to sample undisturbed water.

What has been obtained from this procedure are the towed vehicle longitudinal transfer functions, motion spectra, significant motions, as well as total significant motions.

RESULTS

Tables 1 through 4 show the tow system configuration (vehicle depth, speed, trailback, scope and vehicle pitch) for each vehicle analyzed. Also, control surface deflections are shown when applicable. These tow configurations are those which yield the particular vehicle transfer functions.

Significant vehicle longitudinal motions (surge, heave and pitch) for each vehicle and tow configuration are presented in Tables 5 through 8. While total significant motions are presented in Table 9.

Appendix B contains plots of the tow ship heave spectra, transfer function and resulting vehicle motion spectra, for the longitudinal case. Also contained are lateral motion (roll, yaw and sway) transfer functions for each case.

TABLE 1

VEHICLE A, SYSTEM TOW CONFIGURATION

RUN	DEPTH (ft)	TOW SPEED (kt)	TRAILBACK (ft)	SCOPE (ft)	PITCH (deg)
1	30	2.5	3.24	30.2	0.6
2	30	5.0	13.1	30.7	0.1
3	30	8.0	37.7	48.0	-0.1
4	500	2.5	554.0	778.0	0.6
5	500	5.0	2192.0	2273.0	0.1
6	500	8.0	4165.0	4203.0	-0.1
7	1000	2.5	1683.0	2018.0	0.6
8	1000	5.0	4874.0	5003.0	0.1
9	1000	8.0	8661.0	8728.0	-0.1
10	1500	2.5	2940.0	3383.0	0.6
11	1500	5.0	7581.0	7758.0	0.1
12	1500	8.0	13217.0	13313.0	-0.1

TABLE 2

VEHICLE B, SYSTEM TOW CONFIGURATIONS

RUN	DEPTH (ft)	TOW SPEED (kt)	TRAILBACK (ft)	SCOPE (ft)	PITCH (deg)	DEPRESSOR DEFL.(deg)	DIVE PLANE DEFL. (deg)
13	30	2.5	7.0	31.0	-6.2	10	15
14	30	5.0	7.0	31.0	-8.7	10	15
15	30	8.0	9.0	32.0	-6.6	10	0
16	500	2.5	1488.0	1675.0	4.3	0	0
17	500	5.0	1779.0	1868.0	-3.6	0	0
18	500	8.0	2413.0	2500.0	-6.6	10	0
19	1000	2.5	1377.0	1740.0	-6.21	10	15
20	1000	5.0	2550.0	2812.0	-8.7	10	15
21	1000	8.0	3572.0	3800.0	-9.2	10	15
22	1500	2.5	2288.0	2786.0	-6.2	10	15
23	1500	5.0	4604.0	4929.0	-8.7	10	15
24	1500	8.0	7031.0	7295.0	-9.2	10	15

TABLE 3

VEHICLE C, SYSTEM TOW CONFIGURATIONS

RUN	DEPTH (ft)	TOW SPEED (kt)	TRAILBACK (ft)	SCOPE (ft)	PITCH (deg)	DEPRESSOR DEFL. (deg)
25	30	2.5	8.7	31.0	14.8	-14.0
26	30	5.0	36.8	48.2	4.6	-14.0
27	30	8.0	36.6	48.3	1.4	-12.0
28	500	2.5	593.0	795.0	14.8	-14.0
29	500	5.0	917.0	1091.0	0.8	0.0
30	500	8.0	1415.0	1555.0	-1.9	0.0
31	1000	2.5	1499.0	1843.0	14.3	-12.0
342	1000	5.0	2474.0	2755.0	-1.1	8.0
33	1000	8.0	3148.0	3400.0	-5.2	14.0
34	1500	2.5	2219.0	2752.0	12.4	-4.0
35	1500	5.0	4289.0	4656.0	-2.5	14.0
36	1500	8.0	6764.0	7048.0	-5.3	14.0

TABLE 4

VEHICLE D, SYSTEM TOW CONFIGURATIONS

RUN	DEPTH (ft)	TOW SPEED (kt)	TRAILBACK (ft)	SCOPE (ft)	PITCH (deg)	DIVE PLANE DEFL. (deg)
37	30	2.5	3.3	30.2	4.8	14.0
38	30	5.0	5.8	30.6	6.9	14.0
39	30	8.0	7.1	30.9	7.5	14.0
40	500	2.5	317.0	608.0	8.2	0.0
41	500	5.0	956.0	1124.0	121.4	0.0
42	500	8.0	1743.0	1866.0	12.3	0.0
43	1000	2.5	1054.0	1504.0	8.2	0.0
44	1000	5.0	3101.0	3329.0	11.4	0.0
45	1000	8.0	5443.0	5600.0	12.3	0.0
46	1500	2.5	1970.0	2555.0	8.2	0.0
47	1500	5.0	5331.0	5617.0	11.4	0.0
48	1500	8.0	9189.0	9377.0	12.3	0.0

TABLE 5

SIGNIFICANT LONGITUDINAL MOTIONS FOR VEHICLE A

TOW SPEED (Knots)	SIGNIFICANT MOTION (ft or deg)	DEPTH (ft) 30	500	1000	1500
2.5	X	1.5	0.8	0.5	0.3
	Z	1.4	0.2	0.1	0.1
	Θ	10.4	1.4	0.8	0.7
5.0	X	3.2	1.5	1.5	1.7
	Z	1.9	0.3	0.3	0.8
	Θ	8.0	1.1	1.1	2.6
8.0	X	3.8	1.3	1.8	1.9
	Z	3.2	1.3	1.2	1.1
	Θ	7.7	2.2	2.2	2.0

TABLE 6

SIGNIFICANT LONGITUDINAL MOTIONS FOR VEHICLE B

TOW SPEED (Knots)	SIGNIFICANT MOTION (ft or deg)	DEPTH (ft) 30	500	1000	1500
2.5	X	16.6	0.4	0.2	0.2
	Z	1.8	0.0	0.1	0.1
	θ	30.8	0.0	1.0	0.8
5.0	X	6.8	1.3	0.2	0.2
	Z	2.7	0.3	0.1	0.1
	θ	9.4	0.0	0.6	0.5
8.0	X	11.9	0.2	0.2	0.2
	Z	2.7	0.1	0.0	0.1
	θ	12.1	0.9	0.4	0.4

TABLE 7

SIGNIFICANT LONGITUDINAL MOTIONS FOR VEHICLE C

TOW SPEED (Knots)	SIGNIFICANT MOTION (ft or deg)	DEPTH (ft) 30	500	1000	1500
2.5	X	2.0	0.3	0.3	0.2
	Z	1.5	0.3	0.2	0.1
	Θ	8.0	0.4	0.0	0.6
5.0	X	1.7	0.5	0.2	0.1
	Z	0.4	0.2	0.1	0.1
	Θ	1.0	1.2	0.7	0.5
8.0	X	1.8	0.4	0.0	0.1
	Z	0.2	0.2	0.1	0.1
	Θ	0.5	0.6	0.0	0.3

TABLE 8

SIGNIFICANT LONGITUDINAL MOTIONS FOR VEHICLE D

TOW SPEED (Knots)	SIGNIFICANT MOTION (ft or deg)	DEPTH (ft) 30	500	1000	1500
2.5	X	8.0	1.2	0.5	0.4
	Z	1.3	0.4	0.2	0.1
	Θ	14.1	1.2	0.7	0.5
5.0	X	5.4	0.4	0.3	0.3
	X	1.5	0.2	0.2	0.2
	Θ	9.1	0.9	0.9	0.6
8.0	X	3.5	0.3	0.3	0.3
	Z	1.6	0.2	0.2	0.2
	Θ	6.5	0.7	0.6	0.6

TABLE 9

TOTAL SIGNIFICANT LONGITUDINAL MOTIONS (IN FEET)

TOW SPEED (Knots)	DEPTH (ft)	VEHICLE A	B	C	D
2.5	30	3.4	21.1	3.8	9.9
	500	1.1	0.4	0.6	1.7
	1000	0.7	0.4	0.4	0.7
	1500	0.5	0.3	0.4	0.5
5.0	30	5.5	10.3	2.1	7.2
	500	1.8	1.6	0.8	0.7
	1000	1.9	0.3	0.3	0.5
	1500	2.7	0.3	0.2	0.5
8.0	30	7.4	15.6	2.0	5.4
	500	2.6	0.3	0.6	0.6
	1000	3.1	0.2	0.1	0.5
	1500	3.1	0.2	0.2	0.5

CONCLUSIONS

In comparing the total significant longitudinal motions in Table 9 with the permissible motions of Figure 5, one sees that for the majority of the cases the predicted motions are within the permissible level. Figure 5 indicates that a significant motion of 1.3 feet is permissible within the 0.8 to 1.4 rad per second frequency range.

The motions of vehicle A fall above this limit for all but the 2.5 knot deep tows. The other vehicles have motions above the 1.3 foot level only for the shallow (30 foot) tow at all tow speeds, with the exception of vehicle D at 2.5 knots, 500 ft.

Referring to Figure 1, the Western Gear motion compensation device is able to attentuate towed body motions by an order of magnitude or better within the frequency range of interest. By implementing such a device, all but one system will meet the motion requirements. Vehicle B fails only for the shallow (30 foot) tow.

Plots of the tow ship heave spectra, which have been used as inputs, for 2.5, five and eight knots are presented in Appendix B, Figures 6 through 8. Longitudinal towed system transfer functions, response motion spectra along with significant motions are presented for Vehicle A at 2.5, five and eight knots and 30, 500, 1000, and 1500 foot depths in Figures 9 through 14. Some general conclusions can be made by comparing these plots.

The heave transfer functions, which relate tow ship heave to the heave response of Vehicle A, has a value of 1.0 at zero frequency. This indicates that the towed vehicle is able to follow the ship exactly for very low frequencies of heave. At high frequencies the transfer function asymptotically approaches zero, indicating the insensitivity of the vehicle to very high frequency motions. Transfer functions relating towed vehicle pitch and surge response to tow ship heave have zero values at both zero and infinite frequencies.

In comparing the plots of response spectra and transfer functions, several trends are apparent. First of all in the case of towed vehicle heave response, the response amplitude increases with velocity. Also, the transfer function curve shifts slightly to lower values of frequency. For the 30 foot depth case the transfer function curve becomes peaked for the five and eight knot tow. Whereas for the 2.5 knot case, it maintains a near constant value of one until the curve begins to drop toward zero. This trend is not seen for tow depths of 500 feet and greater which could be attributed to the shift of the transfer functions to lower frequencies as depth is increased. Also, response amplitude decreases as tow depth inceases.

Pitch response decreases as velocity increases, and the transfer function agains shifts slightly to lower frequencies. For the 30 foot depth tow the transfer function curve is peaked with a narrowing in bandwidth as velocity increases. As tow depth increases pitch response amplitude tends to decrease.

Towed vehicle surge response increases with velocity and the bandwidth of the transfer fucntion remains essentially constant. An interesting

feature to note here is the second peak of the transfer function curve in the cases of eight knots, 500 through 1500 foot depth and also at five knots, 1500 foot depth. The cause of these second resonance frequencies is not yet known. As tow depth increases surge response amplitude decreases for the 2.5 knot tow and also for the five and eight knot 30 foot tows. However, surge response amplitude increases for the five and eight knot tows between 500 and 1500 foot depths.

In comparing the various towed systems, consideration must be given to the type of sensors to be incorporated, especially the velocimeters. Various sensor systems are more or less sensitive to different body motions than others. For instance, the airfoil type probe is virtually insensitve to velocity perturbations resulting from vehicle surge but highly sensitive to pitch. Also, the vorticity meter developed by T. Stanford at APL-UW is less sensitive to linear perturbations than angular.

Once again it is stated that this analysis yields no insight into the vibrational motion response of the system. These high frequency motions are a result of the system traveling through a viscous medium and, although may be excited by, are not caused by ship motions.

Also, the tow cable itself can largely affect the response of the system. Alterations in cable parameters (diameter, weight, C_D, etc.) vary the shape of the cable catenary which can significantly alter the effects of ship motions felt by the vehicle.

REFERENCES

1. Santora, G. A. and Crane, J., 1985, "Sensor Requirements for Fine-Scale Ocean Microstructure Vehicles," NCSC, Jan 1985.

2. Koeppen, S. H., 1979, "A Study of the Use of A Towed Body for Ocean Fine and Microstructure Measurement," MAR Tech. Rept. No. 226.

3. Dugan, J. P., 1980, "Motion Stabilization for Towed Oceanographic Sensors," Mar. Tech., Proceedings 16th Annual Conf., Oct 1980, pp 529-534.

4. Dale, S. and Henzel, H., 1966, "Dynamic Characteristics of Underwater Cables- Flow induced Vibrations", NADC-AE-6620.

5. Kallio, J. A., 1977, "Seakeeping Trials of the R/V Cape Henlopen," DTNSRDC, Rept. No,. 77/041, July 1977.

6. Dugan, J. P. and Morris, W. D., 1984, "Instrumentation Requirements for Small Scale Towed Temperature Measurements," NRL Memorandum Rept. No. 5288.

7. Osborn, T. R. And Lueck, R. G., 1984, "Turbulence Measurements with a Towed Body", NPS, Feb 1984.

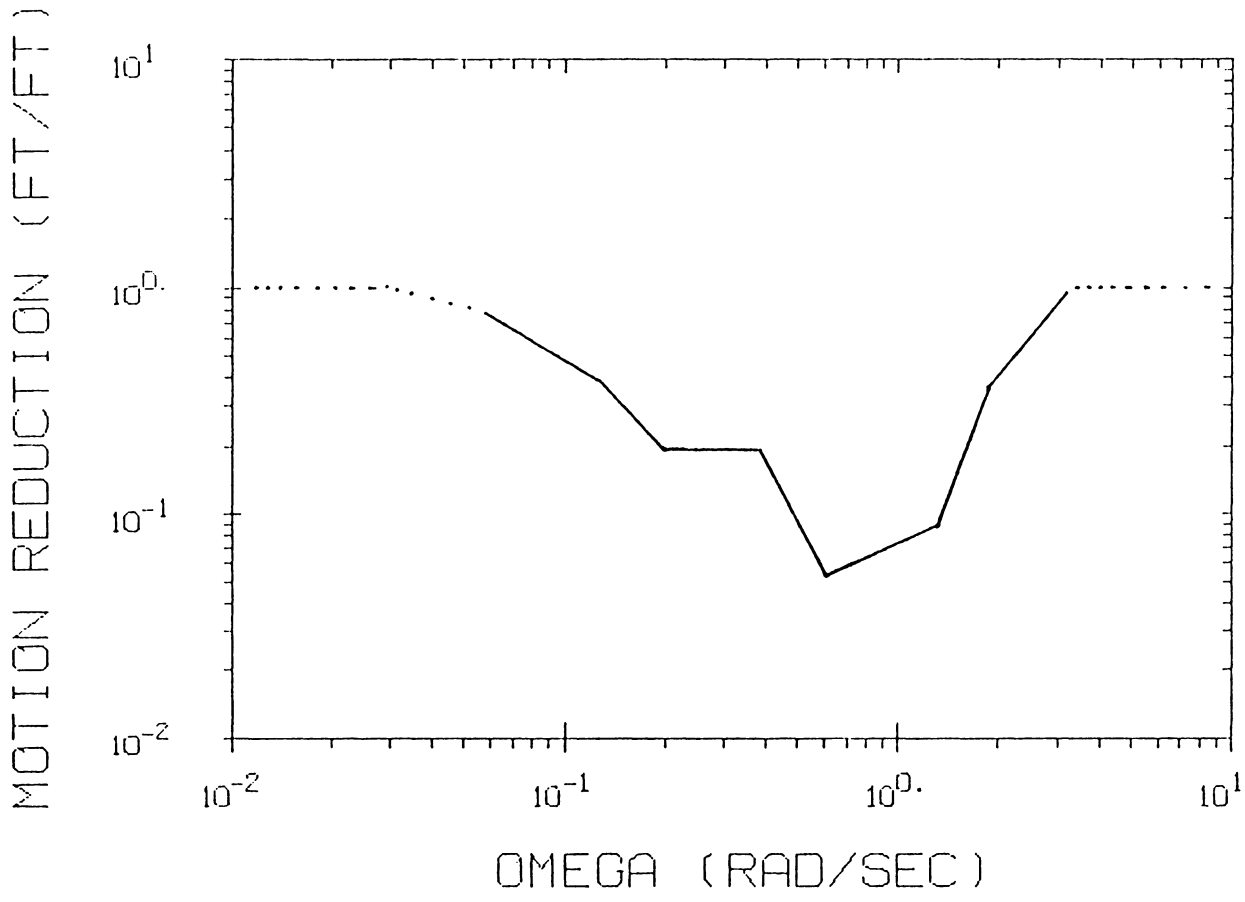

FIGURE 1. ESTIMATED WESTERN GEAR MOTION COMPENSATOR TRANSFER FUNCTION

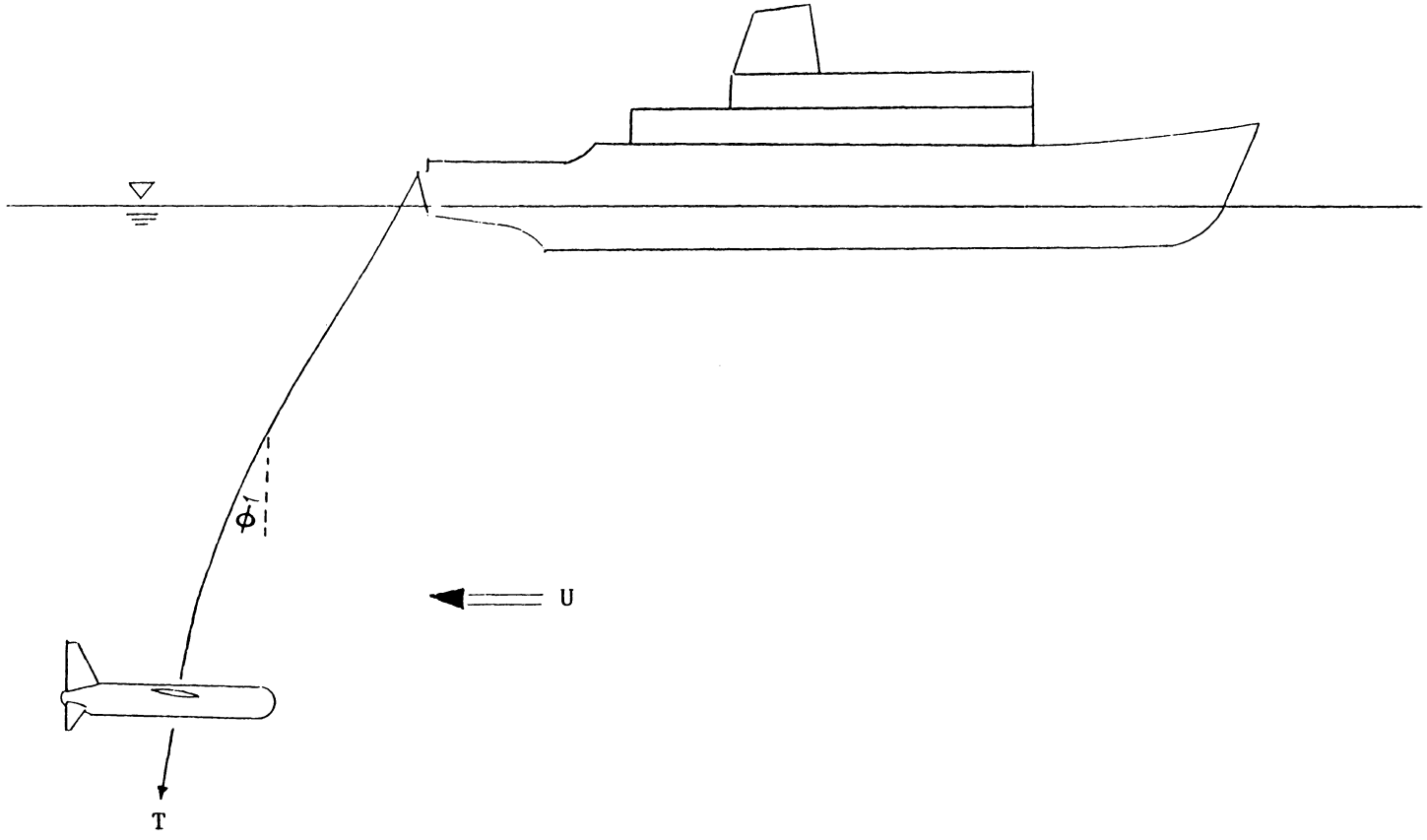

FIGURE 2. TYPICAL TOWED VEHICLE AND CABLE

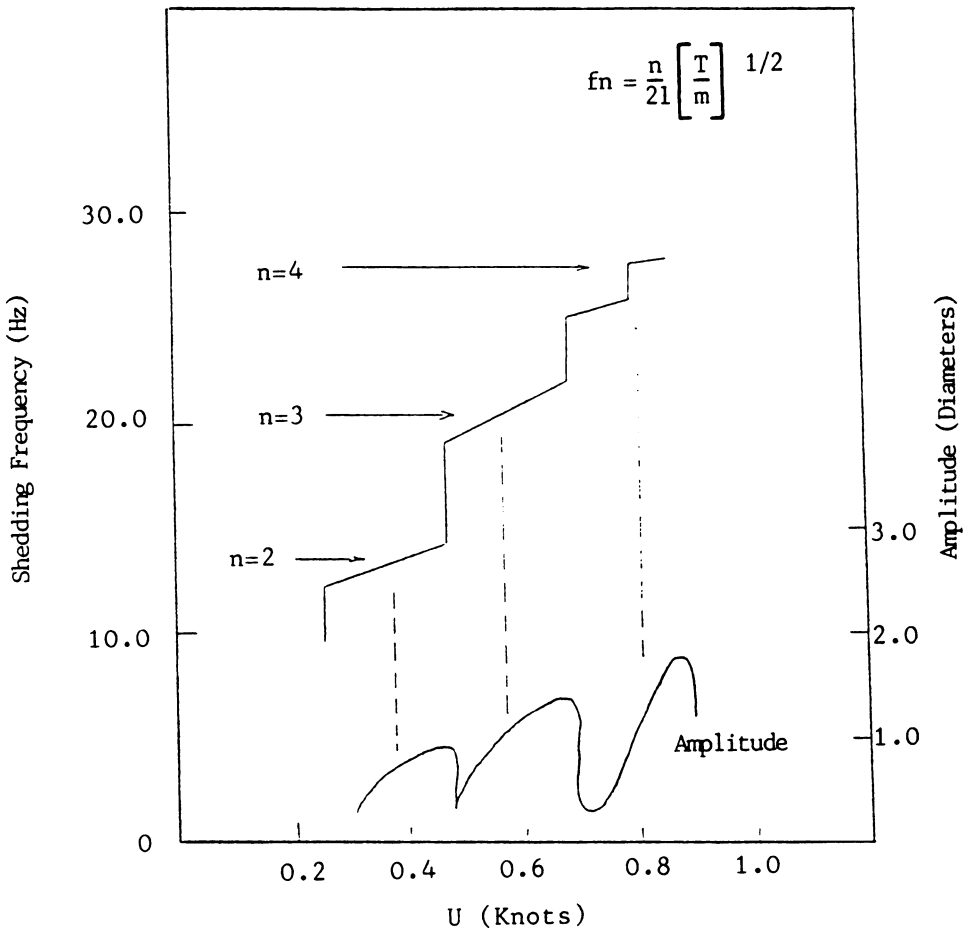

[4]Dale, J. and Henzel, H., (1966), "Dynamic Characteristics of Underwater Cables–Flow Induced Transverse Vibration", NADC–AE–6620.

FIGURE 3. FREQUENCY CHARACTERISTICS FOR A 3.0 FT, 0.1 IN. DIA. CABLE

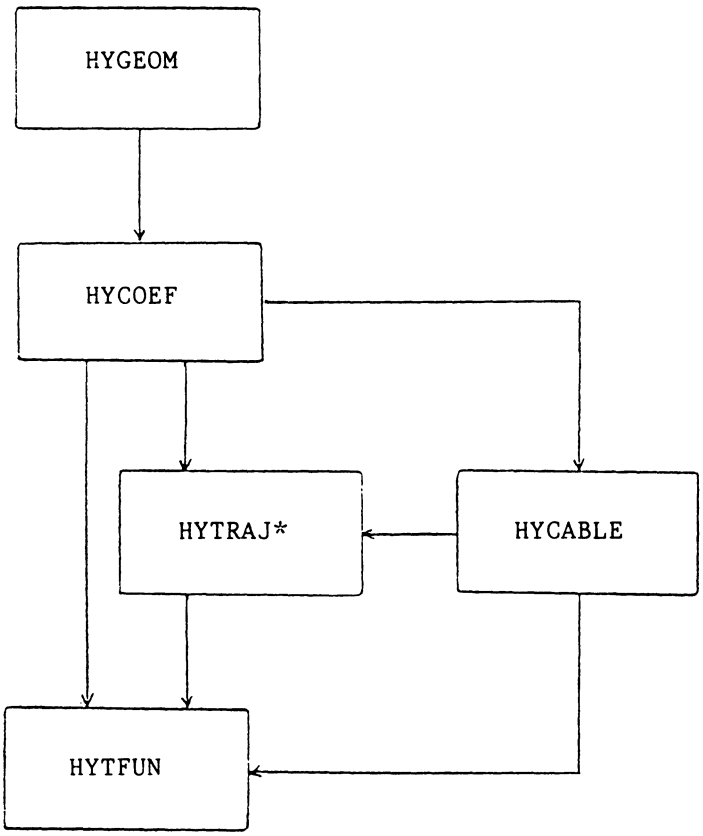

*Indicates this module has not been employed in the present analysis.

FIGURE 4. HYDAT BLOCK DIAGRAM

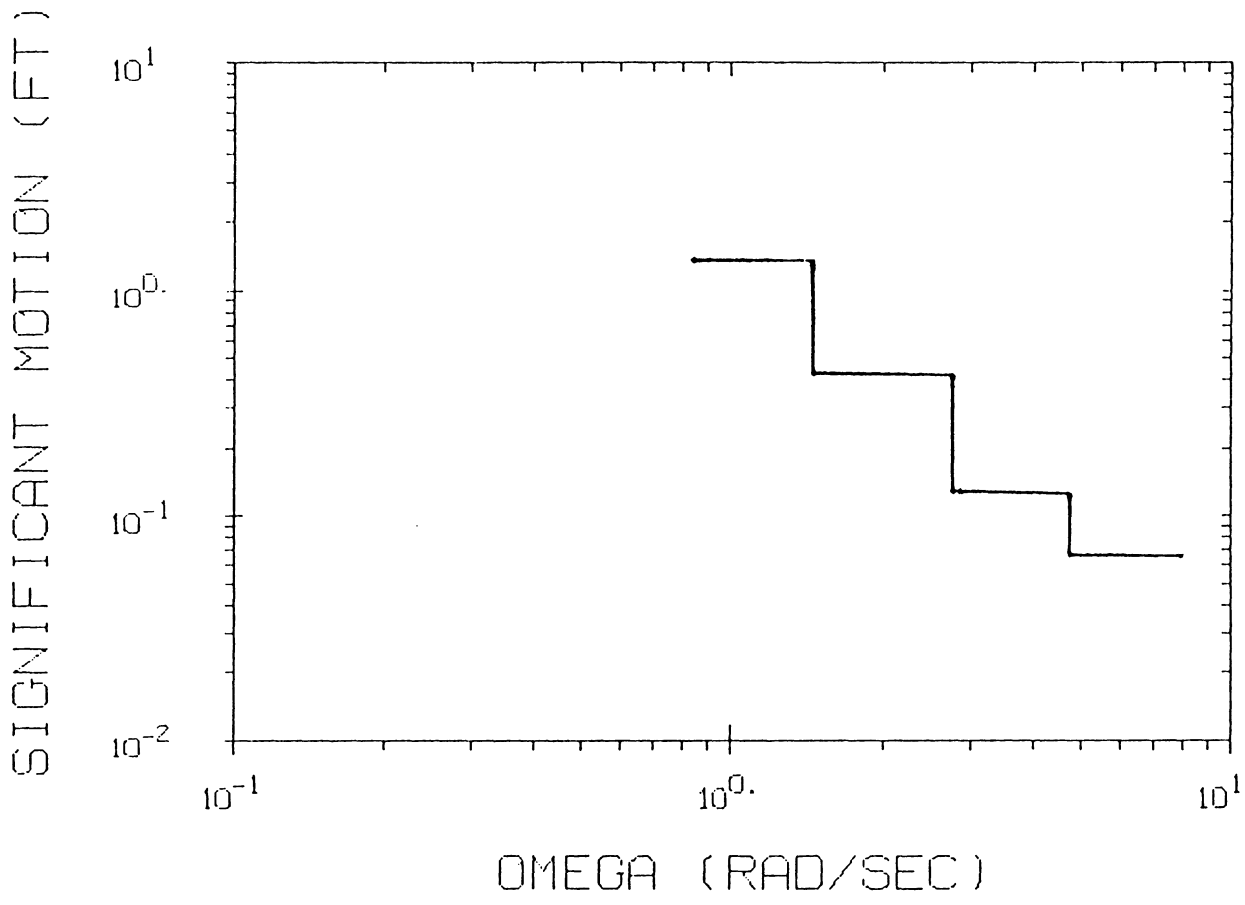

FIGURE 5. PERMISSIBLE VEHICLE MOTIONS

APPENDIX A

LINEARIZED EQUATIONS OF MOTION FOR A TOWED VEHICLE

The equations of motion for a towed vehicle have been linearized for a constant velocity, straight-ahead tow. The terms in the equations have been nondimensionalized by using appropriate combinations of the fluid density ρ, vehicle length ℓ, and the forward speed u_o. The equations have been expressed in matrix form for time domain as

$$\dot{\vec{x}} = A\vec{x} + B\vec{u} + D\vec{v}$$

or for the frequency domain as

$$A(s)\vec{x}(s) + B(s)\vec{u}(s) + D(s)\vec{v}(s) = \vec{0}$$

where A, B, and D are the system, control, and disturbance matrices, and $\vec{x}$, $\vec{u}$, and $\vec{v}$ are the state, control, and disturbance vectors. The longitudinal equations are presented in Table A1, the lateral equations are presented in Table A2 and a complete list of linear hydrodynamic coefficients are presented in Table A3.

NOTATION

Symbol	Dimensionless Form	Definition
CG		Center of mass of vehicle
I_x	$I_x' = \frac{I_x}{\frac{1}{2}\rho\ell^5}$	Moment of inertia of vehicle about x axis
I_y	$I_y' = \frac{I_y}{\frac{1}{2}\rho\ell^5}$	Moment of inertia of vehicle about y axis
I_z	$I_z' = \frac{I_z}{\frac{1}{2}\rho\ell^5}$	Moment of inertia of vehicle about z axis
I_{xy}	$I_{xy}' = \frac{I_{xy}}{\frac{1}{2}\rho\ell^5}$	Product of inertia about xy axis
I_{yz}	$I_{yz}' = \frac{I_{yz}}{\frac{1}{2}\rho\ell^5}$	Product of inertia about yz axis
I_{zx}	$I_{zx}' = \frac{I_{zx}}{\frac{1}{2}\rho\ell^5}$	Product of inertia about zx axis
K	$K' = \frac{K}{\frac{1}{2}\rho\ell^3 U_o^2}$	Hydrodynamic moment component about x axis (rolling moment)
K_p	$K_p' = \frac{K_p}{\frac{1}{2}\rho\ell^4 U_o}$	First order coefficient used in representing K as a function of p
$K_{\dot{p}}$	$K_{\dot{p}}' = \frac{K_{\dot{p}}}{\frac{1}{2}\rho\ell^5}$	Coefficient used in representing K as a function of $\dot{p}$

Symbol	Dimensionless Form	Definition
K_r	$K_r' = \frac{K_r}{\frac{1}{2}\rho \ell^4 U_o}$	First order coefficient used in representing K as a function of r
$K_{\dot{r}}$	$K_{\dot{r}}' = \frac{K_{\dot{r}}}{\frac{1}{2}\rho \ell^5}$	Coefficient used in representing $\dot{K}$ as a function of r
K_v	$K_v' = \frac{K_v}{\frac{1}{2}\rho \ell^3 U_o}$	First order coefficient used in representing K as a function of v
$K_{\dot{v}}$	$K_{\dot{v}}' = \frac{K_{\dot{v}}}{\frac{1}{2}\rho \ell^4}$	Coefficient used in representing $\dot{K}$ as a function of v
K_y	$K_y' = \frac{K_y}{\frac{1}{2}\rho \ell^2 U_o^2}$	Coefficient used in representing K as a function of y
K_{δ_a}	$K_{\delta_a}' = \frac{K_{\delta_a}}{\frac{1}{2}\rho \ell^3 U_o^2}$	First order coefficient used in representing K as a function of δ_a
K_{δ_r}	$K_{\delta_r}' = \frac{K_{\delta_r}}{\frac{1}{2}\rho \ell^3 U_o^2}$	First order coefficient used in representing K as a function of δ_r
K_ψ	$K_\psi' = \frac{K_\psi}{\frac{1}{2}\rho \ell^3 U_o^2}$	Coefficient used in representing K as a function of ψ
K_ϕ	$K_\phi' = \frac{K_\phi}{\frac{1}{2}\rho \ell^2 U_o^2}$	Coefficient used in representing K as a function of ϕ

Symbol	Dimensionless Form	Definition
ℓ	$\ell' = 1$	Overall length of vehicle
m	$m' = \frac{m}{\frac{1}{2}\rho\ell^3}$	Mass of vehicle, including water in free-flooding spaces
M	$M' = \frac{M}{\frac{1}{2}\rho\ell^3 U_o^2}$	Hydrodynamic moment component about y axis (pitching moment)
M_q	$M_q' = \frac{M_q}{\frac{1}{2}\rho\ell^4 U_o}$	First order coefficient used in representing M as a function of q
$M_{\dot{q}}$	$M_{\dot{q}}' = \frac{M_{\dot{q}}}{\frac{1}{2}\rho\ell^5}$	Coefficient used in representing M as a function of $\dot{q}$
M_u	$M_u' = \frac{M_u}{\frac{1}{2}\rho\ell^2 U_o}$	First order coefficient used in representing M as a function of u
$M_{\dot{u}}$	$M_{\dot{u}}' = \frac{M_{\dot{u}}}{\frac{1}{2}\rho\ell^4}$	Coefficient used in representing M as a function of $\dot{u}$
M_w	$M_w' = \frac{M_w}{\frac{1}{2}\rho\ell^3 U_o}$	First order coefficient used in representing M as a function of w
$M_{\dot{w}}$	$M_{\dot{w}}' = \frac{M_{\dot{w}}}{\frac{1}{2}\rho\ell^4}$	Coefficient used in representing M as a function of $\dot{w}$
M_z	$M_z' = \frac{M_z}{\frac{1}{2}\rho\ell U_o^2}$	Coefficient used in representing M as a function of z

Symbol	Dimensionless Form	Definition
M_θ	$M_\theta' = \frac{M_\theta}{\frac{1}{2}\rho \ell^3 U_o^2}$	Coefficient used in representing M as a function of the product θ
M_{δ_b}	$M_{\delta_b}' = \frac{M_{\delta_b}}{\frac{1}{2}\rho \ell^3 U_o^2}$	First order coefficient used in representing M as a function of δ_b
M_{δ_s}	$M_{\delta_s}' = \frac{M_{\delta_s}}{\frac{1}{2}\rho \ell^3 U_o^2}$	First order coefficient used in representing M as a function of δ_s
N	$N' = \frac{N}{\frac{1}{2}\rho \ell^3 U_o^2}$	Hydrodynamic moment component about z axis (yawing moment)
N_p	$N_p' = \frac{N_p}{\frac{1}{2}\rho \ell^4 U_o}$	First order coefficient used in representing N as a function of p
$N_{\dot{p}}$	$N_{\dot{p}}' = \frac{N_{\dot{p}}}{\frac{1}{2}\rho \ell^5}$	Coefficient used in representing N as a function of $\dot{p}$
N_r	$N_r' = \frac{N_r}{\frac{1}{2}\rho \ell^4 U_o}$	First order coefficient used in representing N as a function of r
$N_{\dot{r}}$	$N_{\dot{r}}' = \frac{N_{\dot{r}}}{\frac{1}{2}\rho \ell^5}$	Coefficient used in representing N as a function of $\dot{r}$
N_v	$N_v' = \frac{N_v}{\frac{1}{2}\rho \ell^3 U_o}$	First order coefficient used in representing N as a function of v

Symbol	Dimensionless Form	Definition
$N_{\dot{v}}$	$N_{\dot{v}}' = \frac{N_{\dot{v}}}{\frac{1}{2}\rho\ell^4}$	Coefficient used in representing $\dot{N}$ as a function of $\dot{v}$
N_y	$N_y' = \frac{N_y}{\frac{1}{2}\rho\ell U_o^2}$	Coefficient used in representing N as a function of the product y
N_{δ_a}	$N_{\delta_a}' = \frac{N_{\delta_a}}{\frac{1}{2}\rho\ell^3 U_o^2}$	First order coefficient used in representing N as a function of δ_a
N_{δ_r}	$N_{\delta_r}' = \frac{N_{\delta_r}}{\frac{1}{2}\rho\ell^3 U_o^2}$	First order coefficient used in representing N as a function of δ_r
N_ψ	$N_\psi' = \frac{N_\psi}{\frac{1}{2}\rho\ell^3 U_o^2}$	Coefficient used in representing N as a function of the product ψ
N_ϕ	$N_\phi' = \frac{N_\phi}{\frac{1}{2}\rho\ell^3 U_o^2}$	Coefficient used in representing N as a function of the product ϕ
p	$p' = \frac{p\ell}{U_o}$	Angular velocity component about y axis relative to fluid (roll)
$\dot{p}$	$\dot{p}' = \frac{\dot{p}\ell^2}{U_o^2}$	Angular acceleration component about x axis relative to fluid
q	$q' = \frac{q\ell}{U_o}$	Angular velocity component about y axis relative to fluid (pitch)

Symbol	Dimensionless Form	Definition
$\dot{q}$	$\dot{q}' = \frac{\dot{q}\ell^2}{U_o}$	Angular acceleration component about y axis relative to fluid
r	$r' = \frac{r\ell}{U_o}$	Angular velocity component about z axis relative to fluid (yaw)
$\dot{r}$	$\dot{r}' = \frac{\dot{r}\ell^2}{U_o^2}$	Angular acceleration component about z axis relative to fluid
U_o	$U_o' = \frac{U_o}{U_o}$	Linear velocity of origin of body axis relative to fluid
u	$u' = \frac{u}{U_o}$	Component of U in direction of the x axes
$\dot{u}$	$\dot{u}' = \frac{\dot{u}\ell}{U_o^2}$	Time rate of change of u in direction of the x axis
v	$v' = \frac{v}{U_o}$	Component of U in direction of the y axis
$\dot{v}$	$\dot{v}' = \frac{\dot{v}\ell}{U_o^2}$	Time rate of change of v in direction of the y axis
w	$w' = \frac{w}{U_o}$	Component of U in direction of the z axis
$\dot{w}$	$\dot{w}' = \frac{\dot{w}\ell}{U_o^2}$	Time rate of change of w in direction of the z axis

Symbol	Dimensionless Form	Definition
W	$W' = \frac{W}{\frac{1}{2}\rho \ell^2 U_o^2}$	Weight, including water in free flooding spaces
x	$x' = \frac{x}{\ell}$	Longitudingal body axis; also the coordinate of a point relative to the origin of body axes
x_G	$x_G' = \frac{x_G}{\ell}$	The x coordinate of CG
X	$X' = \frac{X}{\frac{1}{2}\rho \ell^2 U_o^2}$	Hydrodynamic force component along x axis (longitudinal, or axial, force)
X_q	$X_q' = \frac{X_q}{\frac{1}{2}\rho \ell^3 U_o}$	First order coefficient used in representing X as a function of q
$X_{\dot{q}}$	$X_{\dot{q}}' = \frac{X_{\dot{q}}}{\frac{1}{2}\rho \ell^4}$	Coefficient used in representing X as a function of the product q
$X_{\dot{u}}$	$X_{\dot{u}}' = \frac{X_{\dot{u}}}{\frac{1}{2}\rho \ell^3}$	Coefficient used in representing X as a function of $\dot{u}$
X_u	$X_u' = \frac{X_u}{\frac{1}{2}\rho \ell^2 U_o}$	First order coefficient used in representing X as a function of u
X_w	$X_w' = \frac{X_w}{\frac{1}{2}\rho \ell^2 U_o}$	First order coefficient used in representing X as a function of w

Symbol	Dimensionless Form	Definition
$X_{\dot{w}}$	$X_{\dot{w}}' = \frac{X_{\dot{w}}}{\frac{1}{2}\rho\ell^3}$	Coefficient used in representing X as a function of the product w
X_x	$X_x' = \frac{X_x}{\frac{1}{2}\rho\ell U_o^2}$	Coefficient used in representing X as a function of the product x
X_z	$X_z' = \frac{X_z}{\frac{1}{2}\rho\ell U_o^2}$	Coefficient used in representing X as a function of the product z
X_{δ_b}	$X_{\delta_b}' = \frac{X_{\delta_b}}{\frac{1}{2}\rho\ell^2 U_o^2}$	First order coefficient used in representing X as a function of δ_b
X_{δ_s}	$X_{\delta_s}' = \frac{X_{\delta_s}}{\frac{1}{2}\rho\ell^2 U_o^2}$	First order coefficient used in representing X as a function of δ_s
y_G	$y_G' = \frac{y_G}{\ell}$	The y coordinate of CG
Y_p	$Y_p' = \frac{Y_p}{\frac{1}{2}\rho\ell^3 U_o}$	First order coefficient used in representing Y as a function of p
$Y_{\dot{p}}$	$Y_{\dot{p}}' = \frac{Y_{\dot{p}}}{\frac{1}{2}\rho\ell^4}$	Coefficient used in representing Y as a function of $\dot{p}$
Y_r	$Y_r' = \frac{Y_r}{\frac{1}{2}\rho\ell^3 U_o}$	First order coefficient used in representing Y as a function of r

Symbol	Dimensionless Form	Definition
$Y_{\dot{r}}$	$Y_{\dot{r}}' = \frac{Y_{\dot{r}}}{\frac{1}{2}\rho\ell^4}$	Coefficient used in representing $\dot{Y}$ as a function of r
Y_v	$Y_v' = \frac{Y_v}{\frac{1}{2}\rho\ell^2 U_o}$	First order coefficient used in representing Y as a function of v
$Y_{\dot{v}}$	$Y_{\dot{v}}' = \frac{Y_{\dot{v}}}{\frac{1}{2}\rho\ell^3}$	Coefficient used in representing $\dot{Y}$ as a function of v
Y_y	$Y_y' = \frac{Y_y}{\frac{1}{2}\rho\ell U_o^2}$	Coefficient used in representing Y as a function of the product y
Y_{δ_a}	$Y_{\delta_a}' = \frac{Y_{\delta_a}}{\frac{1}{2}\rho\ell^2 U_o^2}$	First order coefficient used in representing Y as a function of δ_a
Y_{δ_r}	$Y_{\delta_r}' = \frac{Y_{\delta_r}}{\frac{1}{2}\rho\ell^2 U_o^2}$	First order coefficient used in representing Y as a function of δ_r
Y_ψ	$Y_\psi' = \frac{Y_\psi}{\frac{1}{2}\rho\ell^2 U_o^2}$	Coefficient used in representing Y_v as a function of ψ
Y_ϕ	$Y_\phi' = \frac{Y_\phi}{\frac{1}{2}\rho\ell^2 U_o^2}$	Coefficient used in representing Y as a function of the product ϕ

Symbol	Dimensionless Form	Definition
z	$z' = \frac{z}{\ell}$	Normal body axis; also the coordinate of a point relative to the origin of the body axes
z_G	$z_G' = \frac{z_G}{\ell}$	The z coordinate of CG
Z	$Z' = \frac{Z}{\frac{1}{2}\rho\ell^2 U_o^2}$	Hydrodynamic force component along z axis (normal force)
Z_q	$Z_q' = \frac{Z_q}{\frac{1}{2}\rho\ell^3 U_o}$	First order coefficient used in representing Z as a function of q
$Z_{\dot{q}}$	$Z_{\dot{q}}' = \frac{Z_{\dot{q}}}{\frac{1}{2}\rho\ell^4}$	Coefficient used in representing Z as a function of $\dot{q}$
Z_u	$Z_u' = \frac{Z_u}{\frac{1}{2}\rho\ell^2 U_o}$	First order coefficient used in representing Z as a function of u
$Z_{\dot{u}}$	$Z_{\dot{u}}' = \frac{Z_{\dot{u}}}{\frac{1}{2}\rho\ell^3}$	Coefficient used in representing Z as a function of product $\dot{u}$
Z_w	$Z_w' = \frac{Z_w}{\frac{1}{2}\rho\ell^2 U_o}$	First order coefficient used in representing Z as a function of w
$Z_{\dot{w}}$	$Z_{\dot{w}}' = \frac{Z_{\dot{w}}}{\frac{1}{2}\rho\ell^3}$	Coefficient used in representing Z as a function of $\dot{w}$

Symbol	Dimensionless Form	Definition
Z_x	$Z_x' = \frac{Z_x}{\frac{1}{2}\rho \ell U_o^2}$	Coefficient used in representing Z as a function of x
Z_z	$Z_z' = \frac{Z_z}{\frac{1}{2}\rho \ell U_o^2}$	Coefficient used in representing Z as a function of Z
Z_{δ_b}	$Z_{\delta_b}' = \frac{Z_{\delta_b}}{\frac{1}{2}\rho \ell^2 U_o^2}$	First order coefficient used in representing Z as a function of δ_b
Z_{δ_s}	$Z_{\delta_s}' = \frac{Z_{\delta_s}}{\frac{1}{2}\rho \ell^2 U_o^2}$	First order coefficient used in representing Z as a function of δ_s
δ_s		Deflection of Aileron
δ_b		Deflection of bowplane or sailplane
δ_r		Deflection of rudder
δ_s		Deflection of sternplane
θ		Angle of pitch
ψ		Angle of yaw
ϕ		Angle of roll

TABLE A1

LONGITUDINAL LINEAR EQUATIONS OF MOTION

(Sheet 1 of 2)

$$\underset{\text{system}}{A(s)\vec{x}(s)} + \underset{\text{control}}{B(s)\vec{u}(s)} + \underset{\text{disturbances}}{D(s)\vec{v}(s)} = \vec{0}$$

$$A = \begin{bmatrix} (X'_{\dot{u}}-m')s+X'_u & X'_{\dot{w}}+X'_w & (X'_{\dot{q}}-m'z'_G)s+X'_q-m'\sin\theta_o & X'_x & X'_z & X'_\theta \\ Z'_{\dot{u}}s+Z'_u & (Z'_{\dot{w}}-m')s+Z'_w & (Z'_{\dot{q}}+m'x'_G)s+Z'_q+m'\cos\theta_o & Z'_x & Z'_z & Z'_\theta \\ (M'_{\dot{u}}+m'z'_G)s+M'_u & (M'_{\dot{w}}-m'x'_G)s+M'_w & (M'_{\dot{q}}-I'_y)s+M'_q-m'x'_G\cos\theta_o-m'z'_G\sin\theta_o & M'_x & M'_z & M'_\theta \\ -\cos\theta_o & -\sin\theta_o & 0 & s & 0 & 0 \\ \sin\theta_o & -\cos\theta_o & 0 & 0 & s & 1 \\ 0 & 0 & -1 & 0 & 0 & s \end{bmatrix}$$

TABLE A1

LONGITUDINAL LINEAR EQUATIONS OF MOTION

(Sheet 2 of 2)

$$B = \begin{bmatrix} X'_{\delta_s} & X'_{\delta_b} \\ Z'_{\delta_s} & Z'_{\delta_b} \\ M'_{\delta_s} & M'_{\delta_b} \\ 0 & 0 \\ 0 & 0 \end{bmatrix} \qquad D = \begin{bmatrix} X'_x & X'_z \\ Z'_x & Z'_z \\ M'_x & M'_z \\ 0 & 0 \\ 0 & 0 \end{bmatrix}$$

$$\vec{x}(s) = [u', w', q', x', z', \theta]^T$$

$$\vec{u}(s) = [\delta_s, \delta_b]$$

$$\vec{v}(s) = [x'_{TP}, z'_{TP}]^T$$

TABLE A2

LATERAL LINEAR EQUATIONS OF MOTION

(Sheet 1 of 2)

$$
A = \begin{bmatrix}
(Y'_{\dot{v}}-m')s+Y'_v & (Y'_{\dot{p}}+m'z'_G)s+Y'_p+m'\sin\theta_o & (Y'_{\dot{r}}-m'x'_G)s+Y'_r-m'\cos\theta_o & Y'_y & Y'_\phi & Y'_\psi \\
(K'_{\dot{v}}+m'z'_G)s+K'_v & (K'_{\dot{p}}-I'_x)s+K'_p-m'z'_G\sin\theta_o & (K'_{\dot{r}}+I'_{yz})s+K'_r+m'z'_G\cos\theta_o & K'_y & K'_\phi & K'_\psi \\
(N'_{\dot{v}}+m'x'_G)s+N'_v & (N'_{\dot{p}}+I'_{yz})s+N'_p+m'x'_G\sin\theta_o & (N'_{\dot{r}}-I'_z)s+N'_r-m'x'_G\cos\theta_o & N'_y & N'_\phi & N'_\psi \\
-1 & 0 & 0 & s & \sin\theta_o & -1 \\
0 & -1 & -\tan\theta_o & 0 & s & 0 \\
0 & 0 & -\sec\theta_o & 0 & 0 & s
\end{bmatrix}
$$

TABLE A2

LATERAL LINEAR EQUATIONS OF MOTION

(Sheet 2 of 2)

$$B = \begin{bmatrix} Y'_{\delta_r} & Y'_{\delta_a} \\ K'_{\delta_r} & K'_{\delta_r} \\ N'_{\delta_r} & N'_{\delta_a} \\ 0 & 0 \\ 0 & 0 \\ 0 & 0 \end{bmatrix} \qquad D = \begin{bmatrix} Y'_y \\ K'_y \\ N'_y \\ 0 \\ 0 \\ 0 \end{bmatrix}$$

$$\vec{x} = \{v', p', r', y', \phi, \psi\}^T$$

$$\vec{u} = \{\delta_r, \delta_a\}^T$$

$$\vec{v} = \{y'_{TP}\}^T$$

TABLE A3

HYDRODYNAMIC COEFFICIENTS FOR LINEAR STABILITY ANALYSIS

	LINEAR			ROTATIONAL		
Acceleration Coefficients	$X_{\dot{u}}$	$Z_{\dot{u}}$	$M_{\dot{u}}$	$Y_{\dot{v}}$	$N_{\dot{v}}$	$K_{\dot{v}}$
	$X_{\dot{w}}$	$Z_{\dot{w}}$	$M_{\dot{w}}$	$Y_{\dot{r}}$	$N_{\dot{r}}$	$K_{\dot{r}}$
	$X_{\dot{q}}$	$Z_{\dot{q}}$	$M_{\dot{q}}$	$Y_{\dot{p}}$	$N_{\dot{p}}$	$K_{\dot{p}}$
Static Coefficients	X_u	Z_u	M_u	Y_v	N_v	K_v
	X_w	Z_w	M_w			
Dynamic Coefficients	X_q	Z_q	M_q	Y_r	N_r	K_r
				Y_p	N_p	K_p
Gravity - Buoyancy Coefficients	X_θ	Z_θ	M_θ	Y_ϕ	N_ϕ	K_ϕ
Control Coefficients	X_δ	Z_δ	M_δ	Y_δ	N_δ	K_δ
Cable Coefficients	X_x	Z_x	M_x	Y_y	N_y	K_y
	X_z	Z_z	M_z	Y_ϕ	N_ϕ	K_ϕ
	X_θ	Z_θ	M_θ	Y_ψ	N_ψ	K_ψ

APPENDIX B

PLOTS OF SHIP HEAVE SPECTRA, TRANSFER FUNCTIONS

AND LONGITUDINAL MOTION SPECTRA

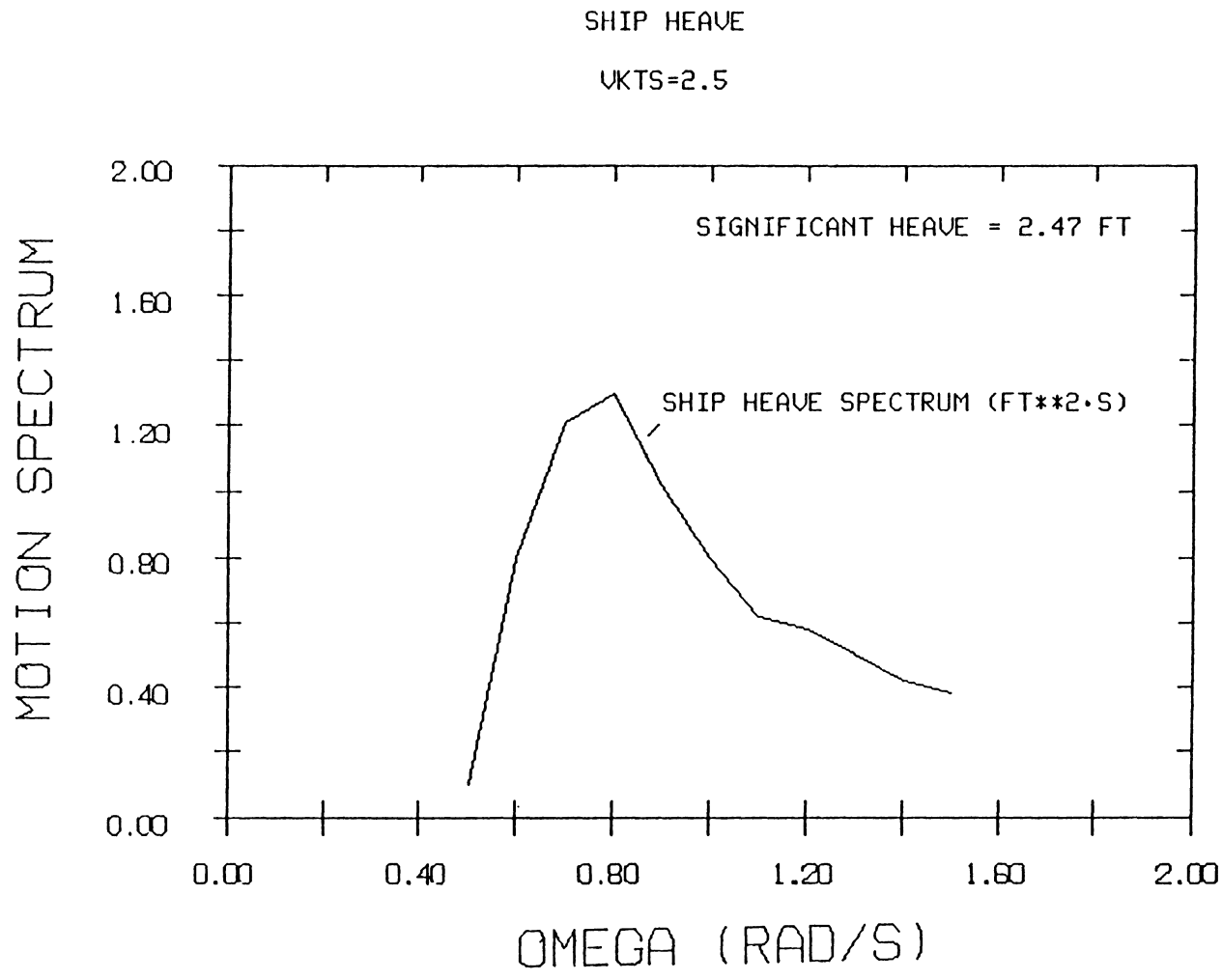

FIGURE 6. TOW SHIP HEAVE SPECTRUM, 2.5 KT

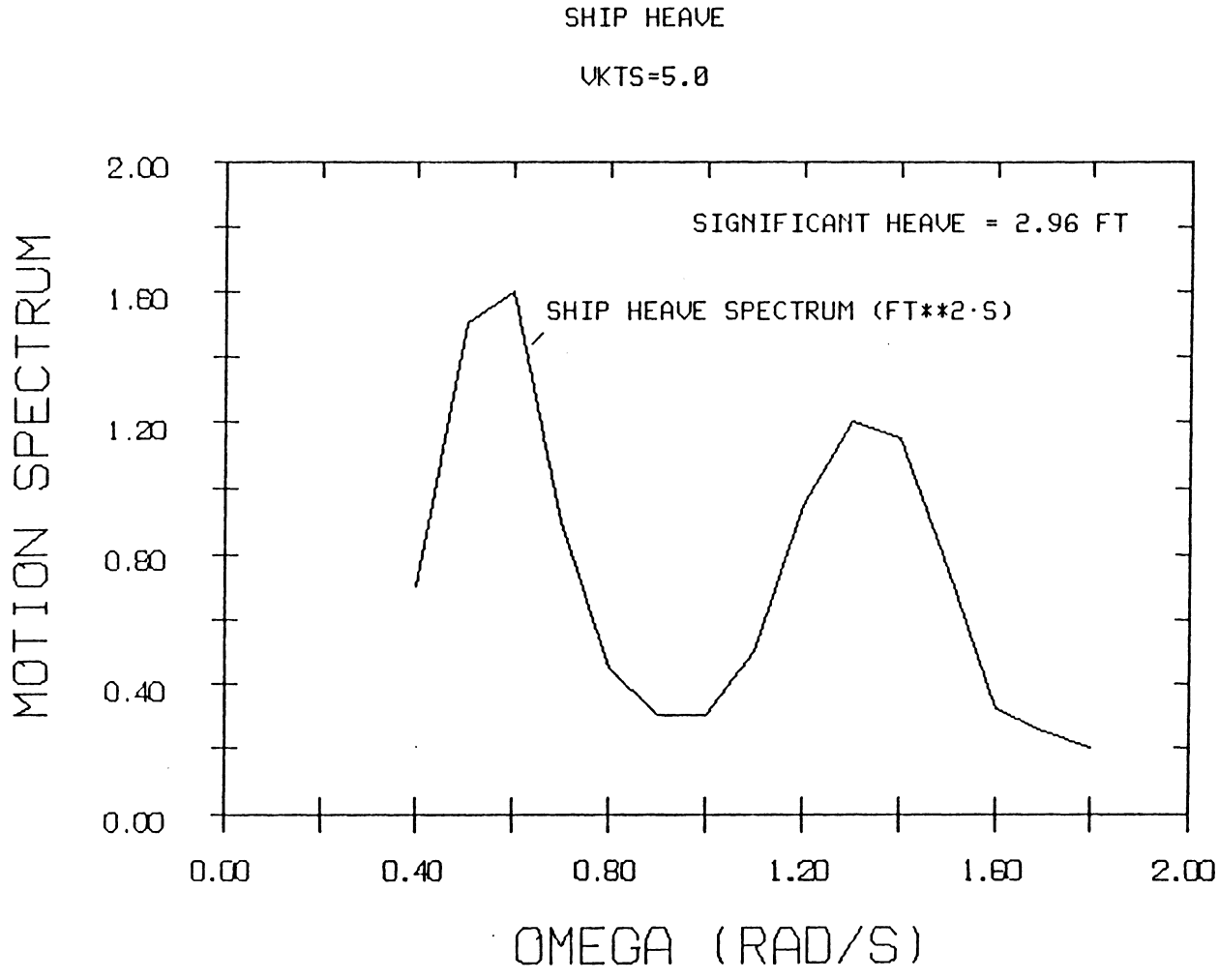

FIGURE 7. TOW SHIP HEAVE SPECTRUM, 5.0 KT

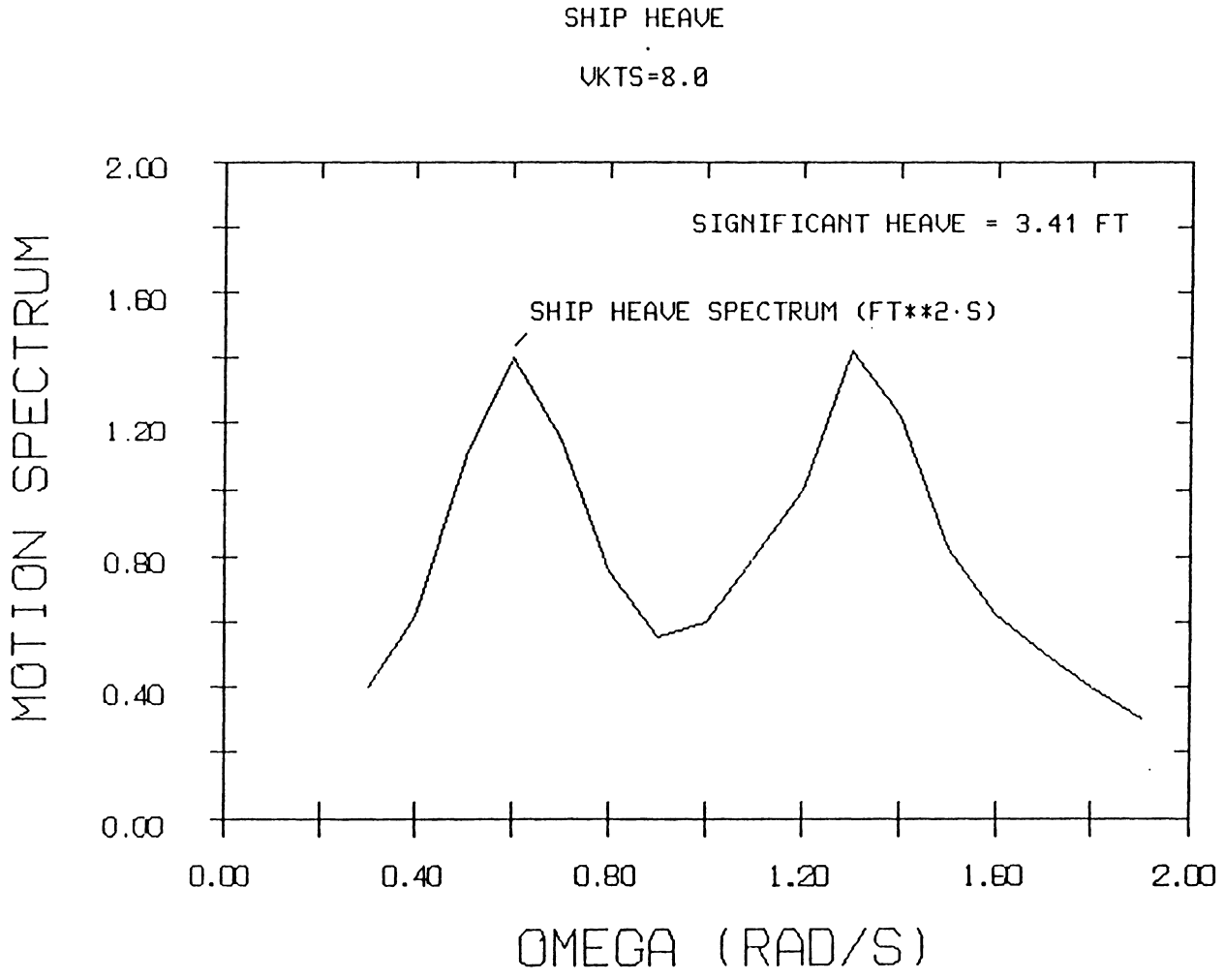

FIGURE 8. TOW SHIP HEAVE SPECTRUM, 8.0 KT

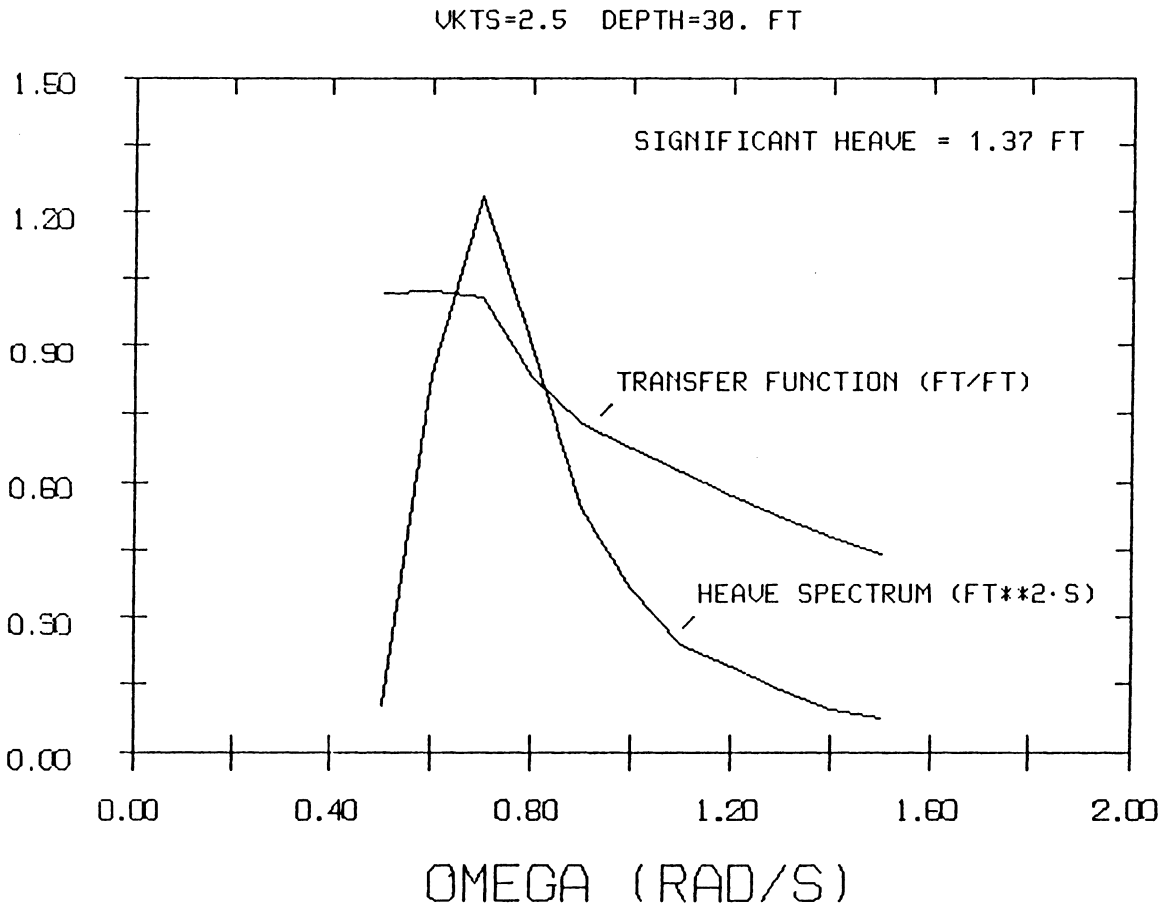

FIGURE 9. TRANSFER FUNCTION AND SPECTRUM (HEAVE) FOR VEHICLE A AT 2.5 KT AND 30 FT DEPTH

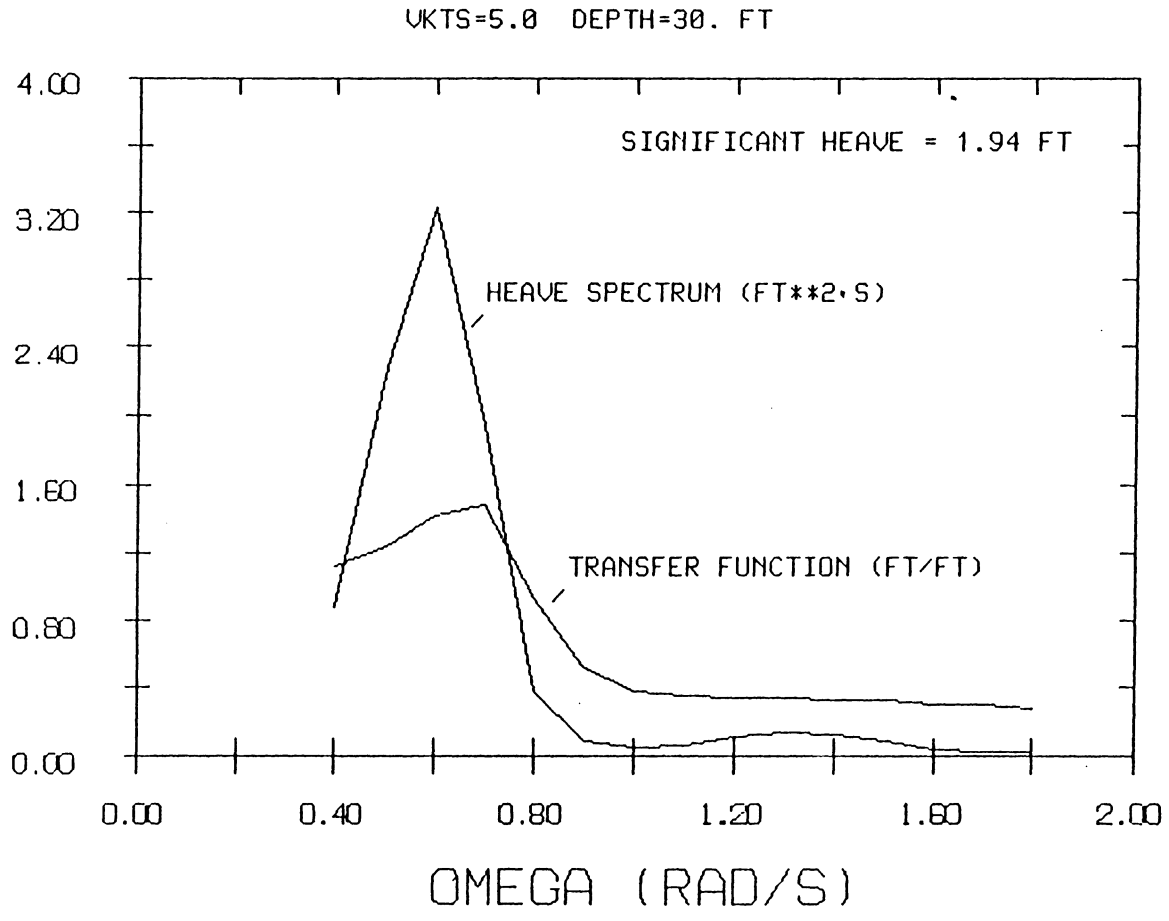

FIGURE 10. TRANSFER FUNCTION AND SPECTRUM (HEAVE) FOR VEHICLE A AT 5.0 KT AND 30 FT DEPTH

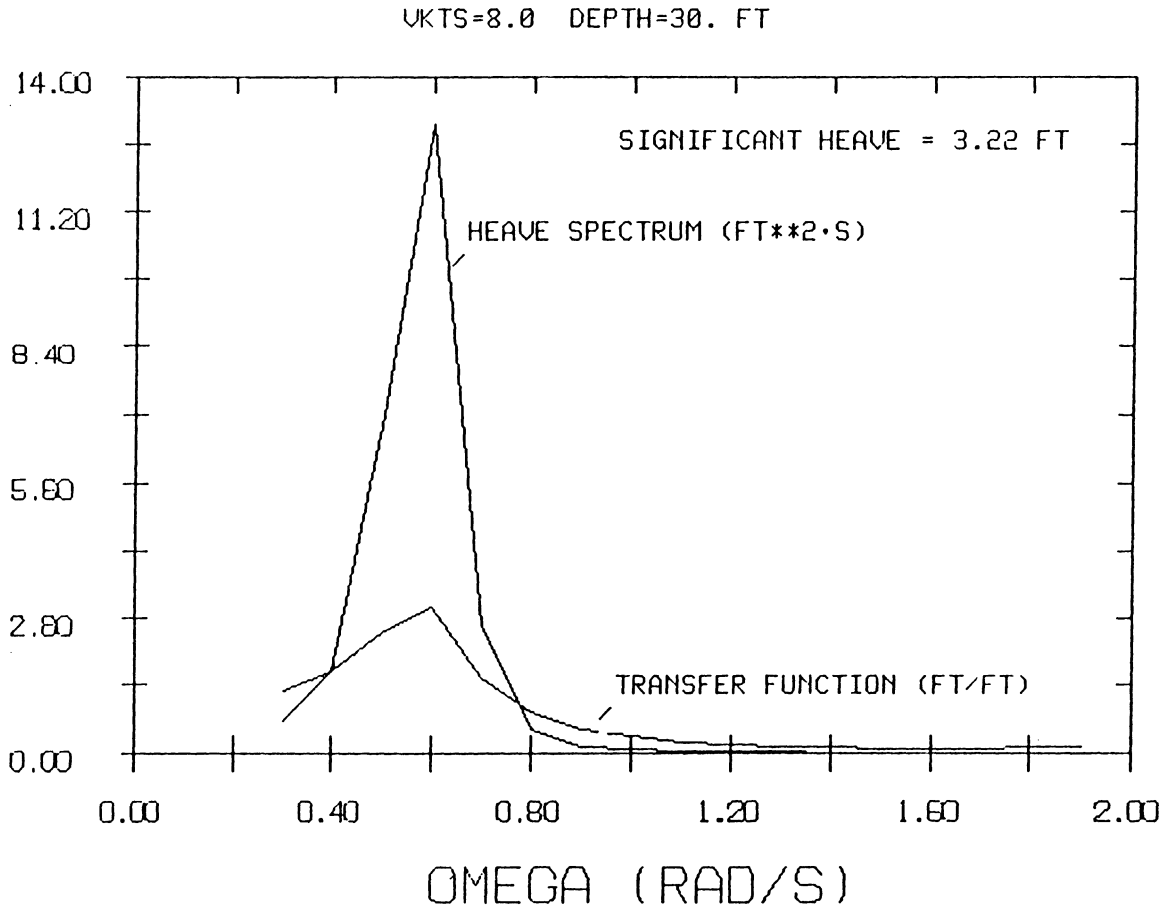

FIGURE 11. TRANSFER FUNCTION AND SPECTRUM (HEAVE) FOR VEHICLE A AT 8.0 KT AND 30 FT DEPTH

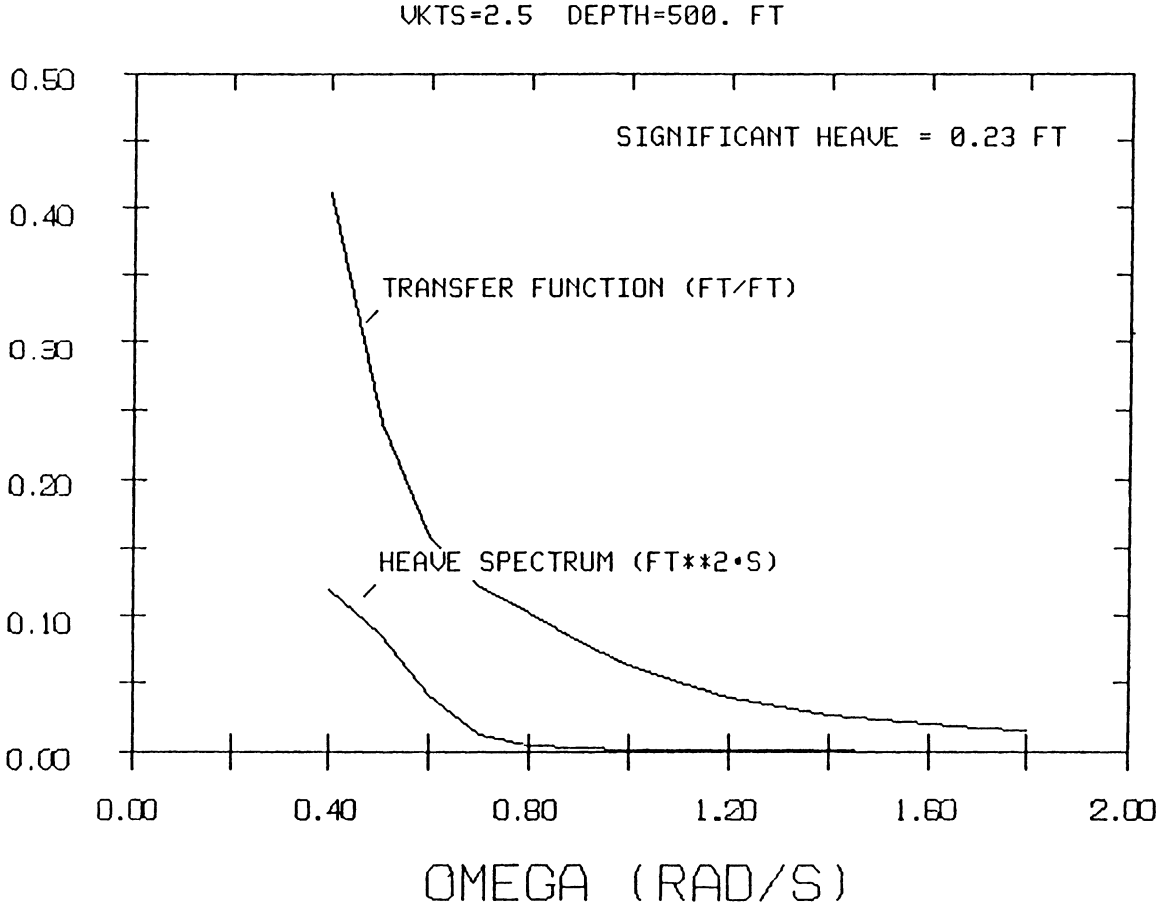

FIGURE 12. TRANSFER FUNCTION AND SPECTRUM (HEAVE) FOR VEHICLE A AT 2.5 KT AND 500 FT DEPTH

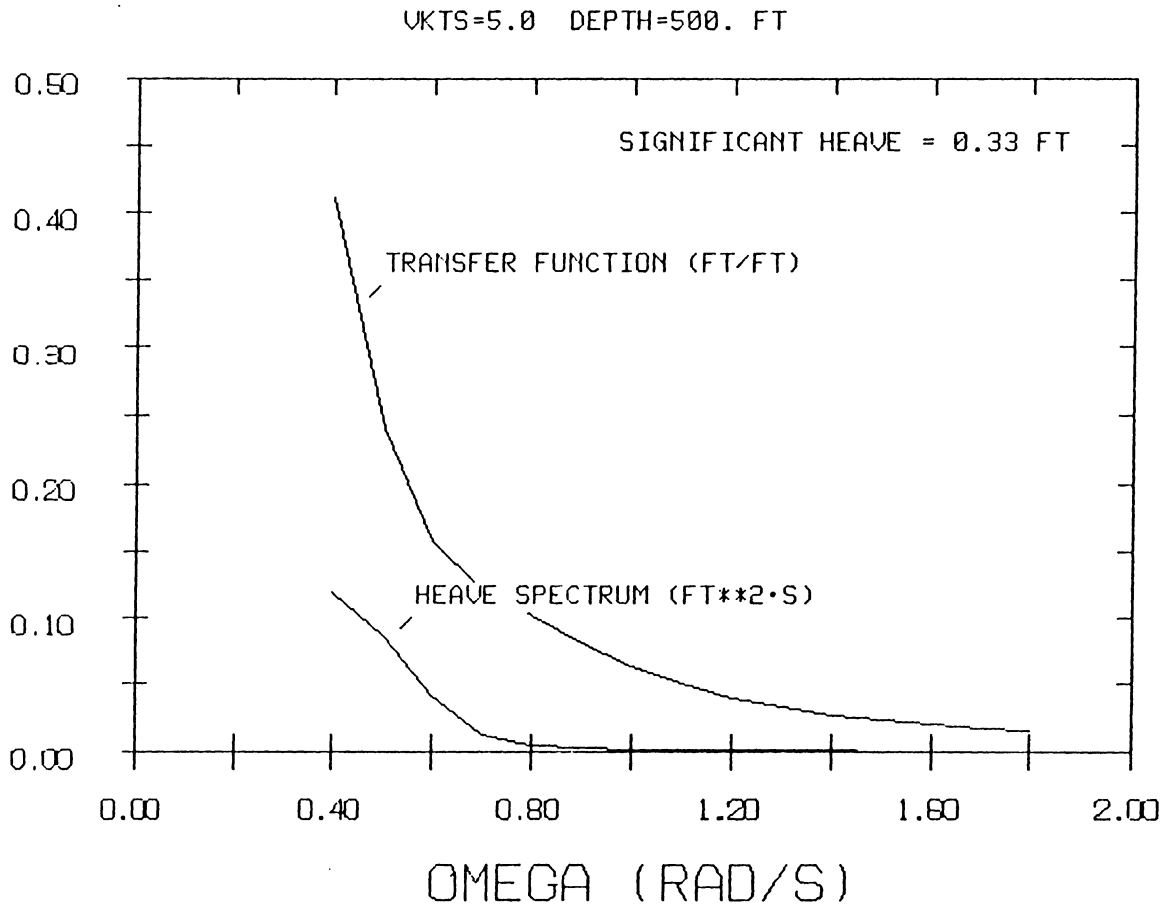

FIGURE 13. TRANSFER FUNCTION AND SPECTRUM (HEAVE) FOR VEHICLE A AT 5.0 KT AND 500 FT DEPTH

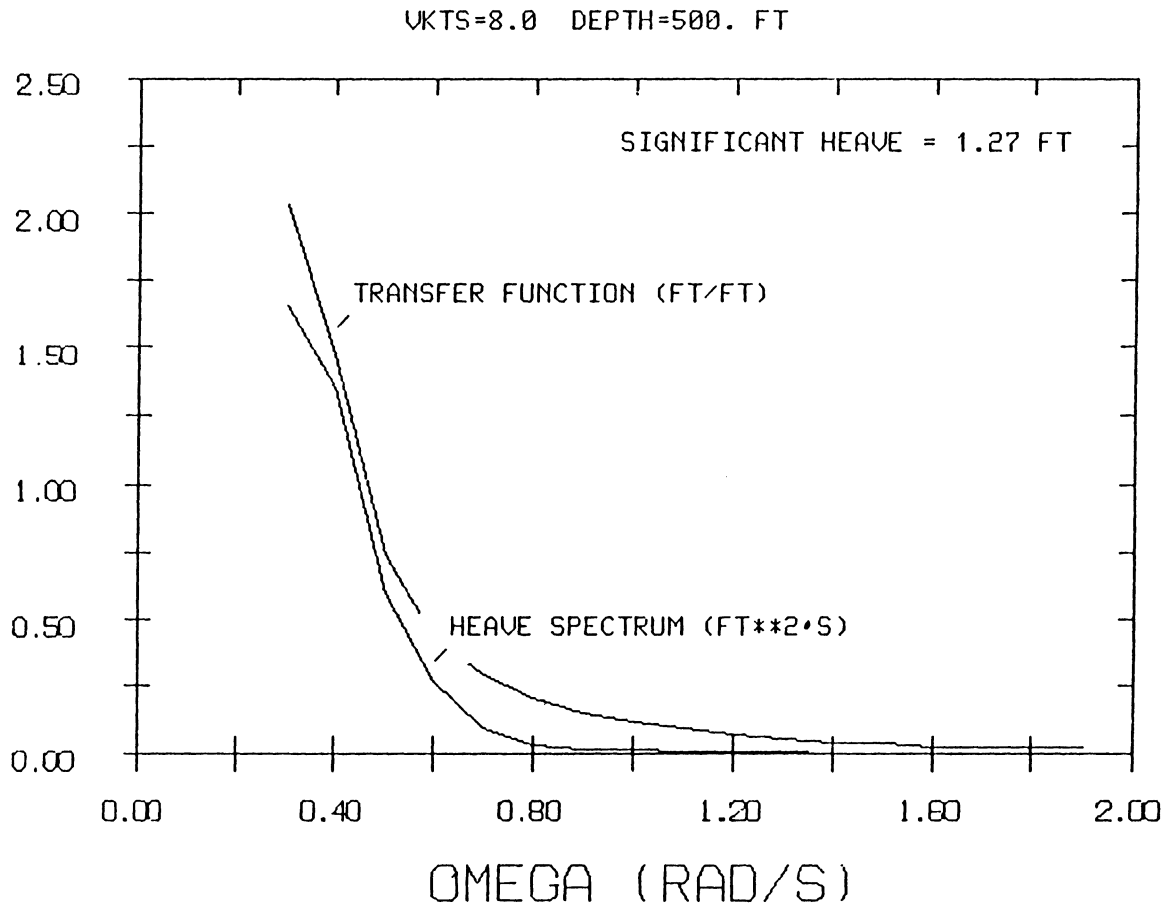

FIGURE 14. TRANSFER FUNCTION AND SPECTRUM (HEAVE) FOR VEHICLE AT 8.0 KT AND 500 FT DEPTH

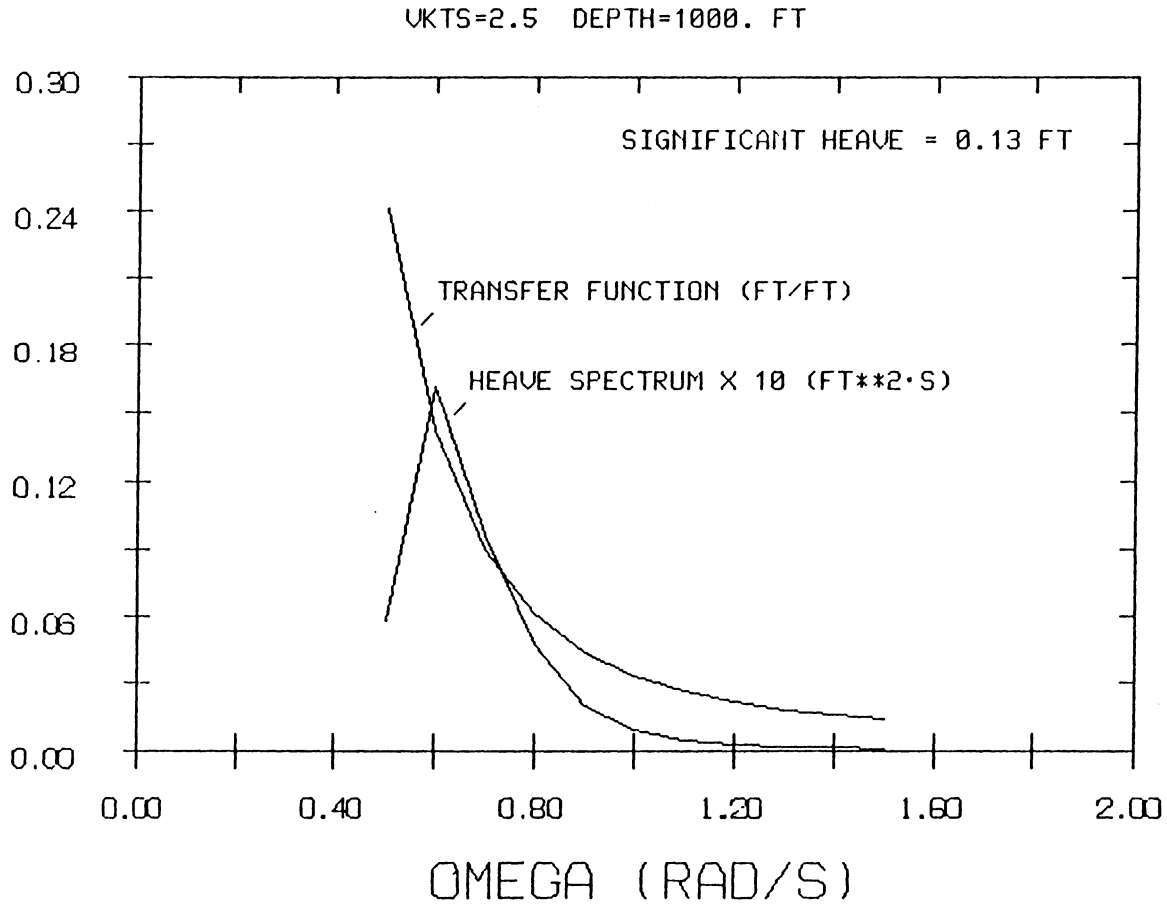

FIGURE 15. TRANSFER FUNCTION AND SPECTRUM (HEAVE) FOR VEHICLE AT 2.5 KT AND 1000 FT DEPTH

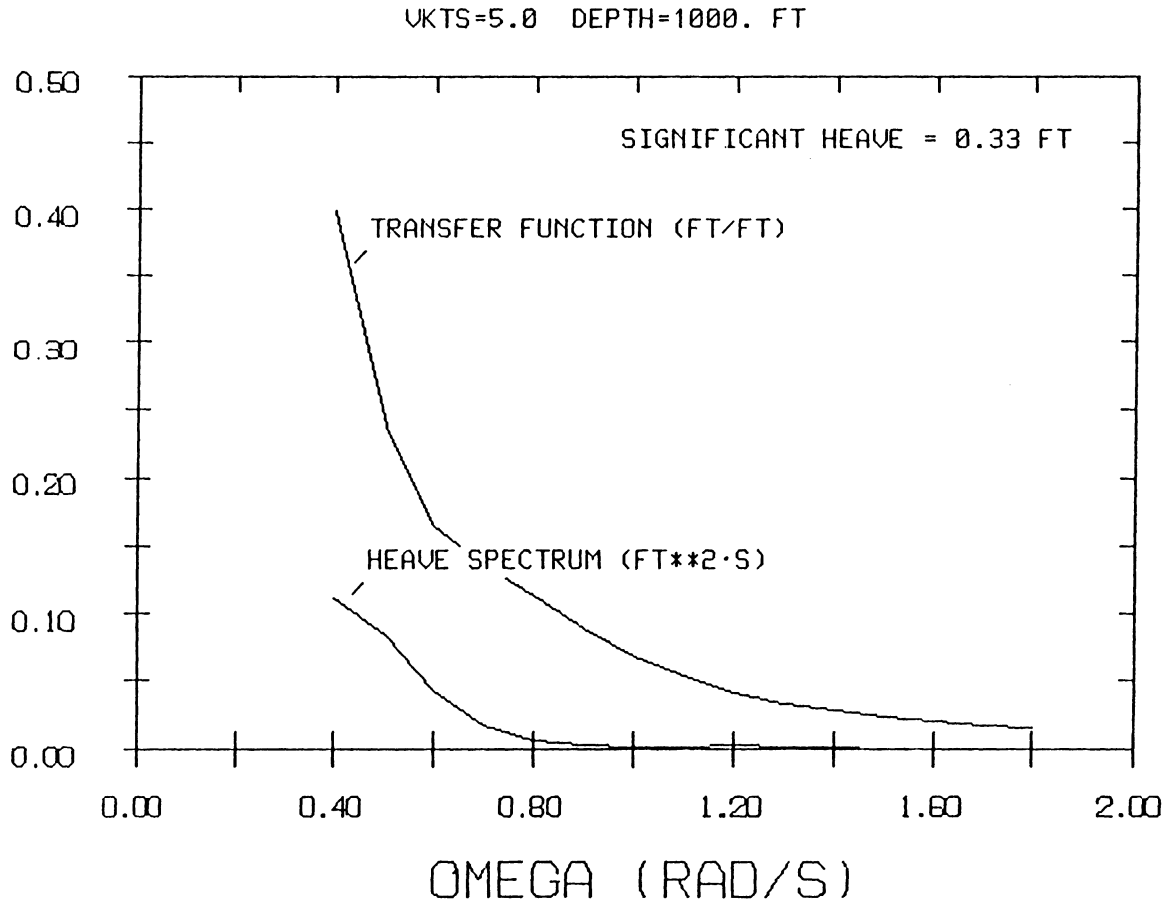

FIGURE 16. TRANSFER FUNCTION AND SPECTRUM (HEAVE) FOR VEHICLE AT 5.0 KT AND 1000 FT DEPTH

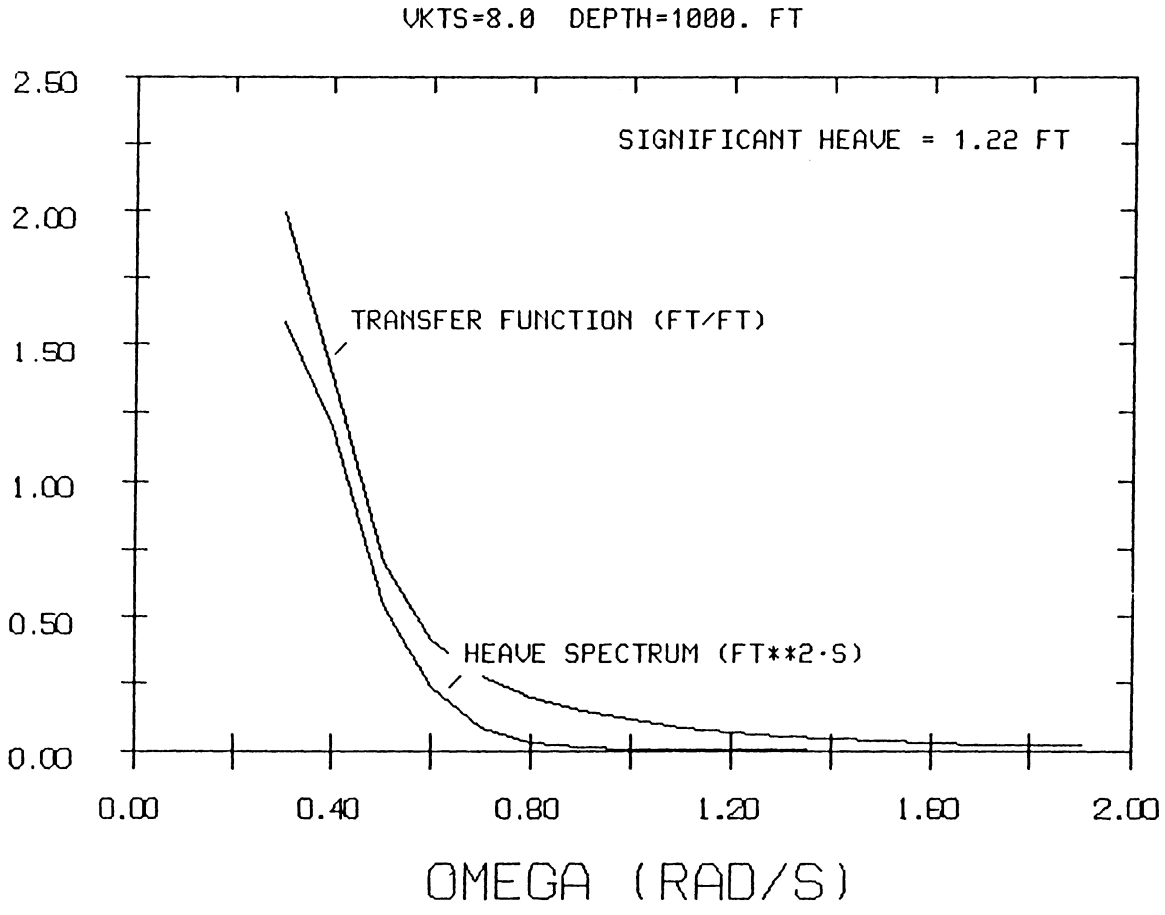

FIGURE 17. TRANSFER FUNCTION AND SPECTRUM (HEAVE) FOR VEHICLE AT 8.0 KT AND 1000 FT DEPTH

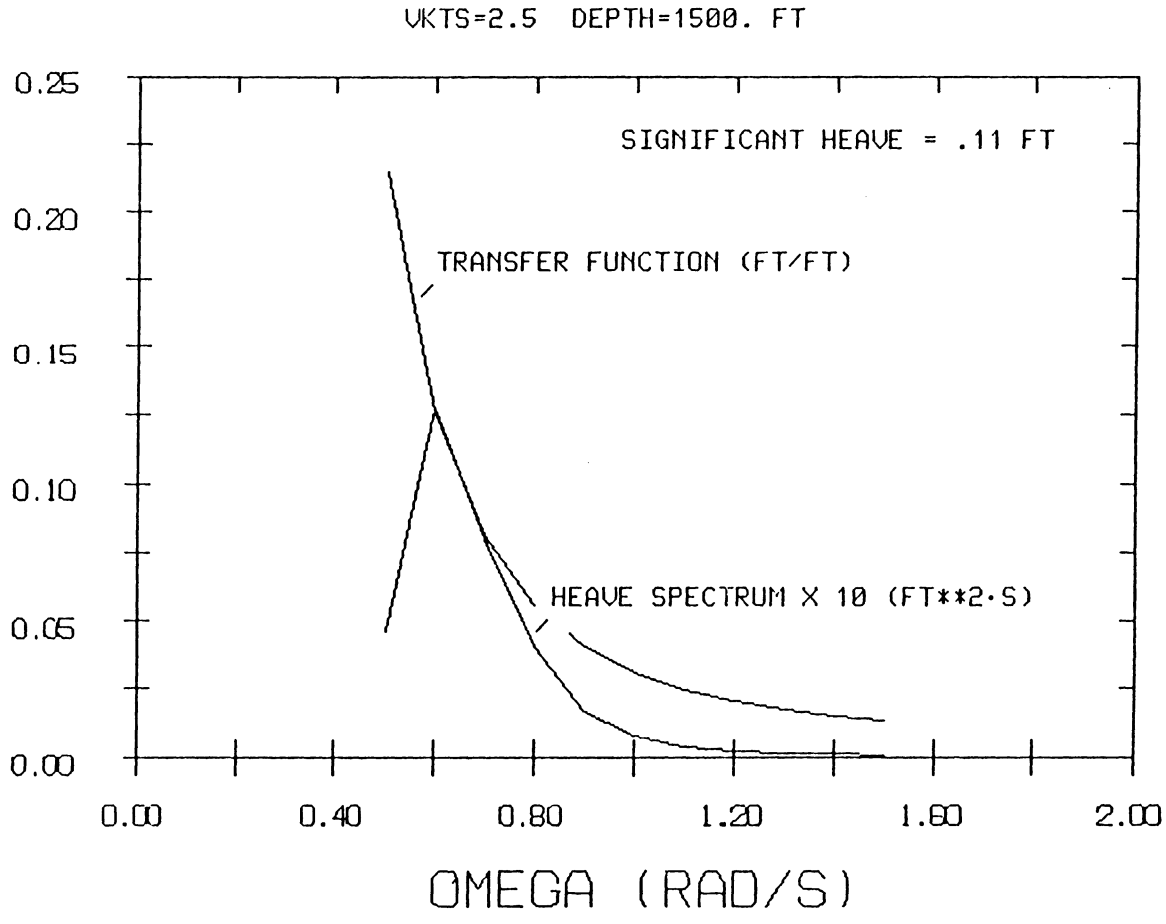

FIGURE 18. TRANSFER FUNCTION AND SPECTRUM (HEAVE) FOR VEHICLE AT 2.5 KT AND 1500 FT DEPTH

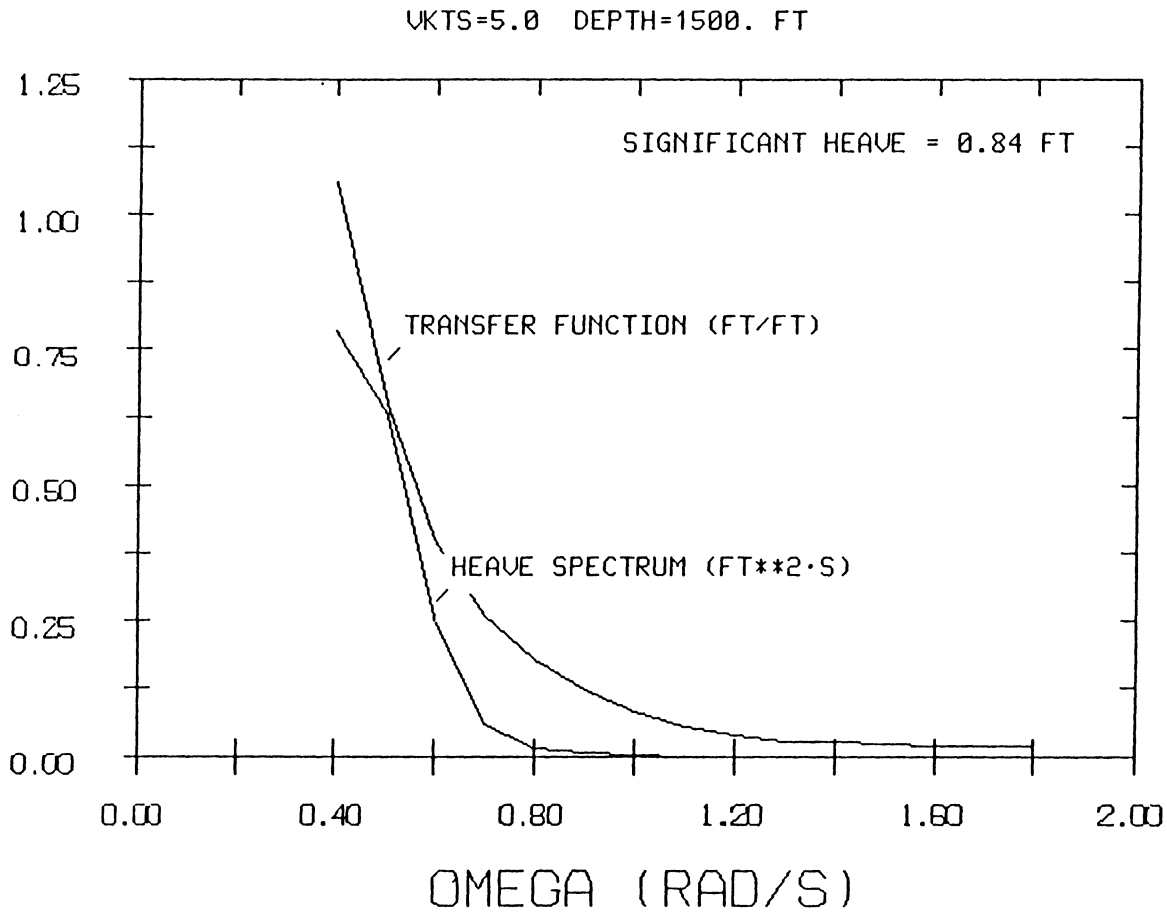

FIGURE 19. TRANSFER FUNCTION AND SPECTRUM (HEAVE) FOR VEHICLE AT 5.0 KT AND 1500 FT DEPTH

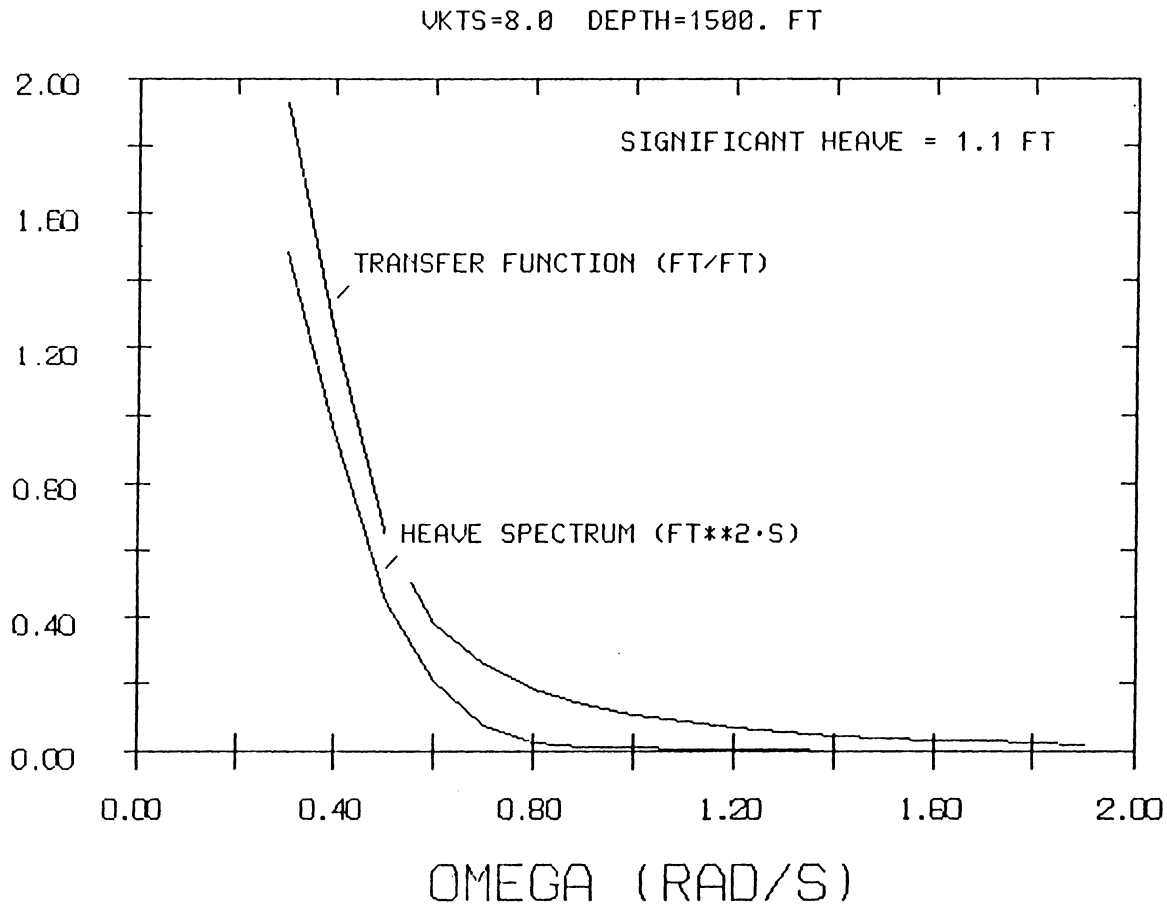

FIGURE 20. TRANSFER FUNCTION AND SPECTRUM (HEAVE) FOR VEHICLE AT 8.0 KT AND 1500 FT DEPTH

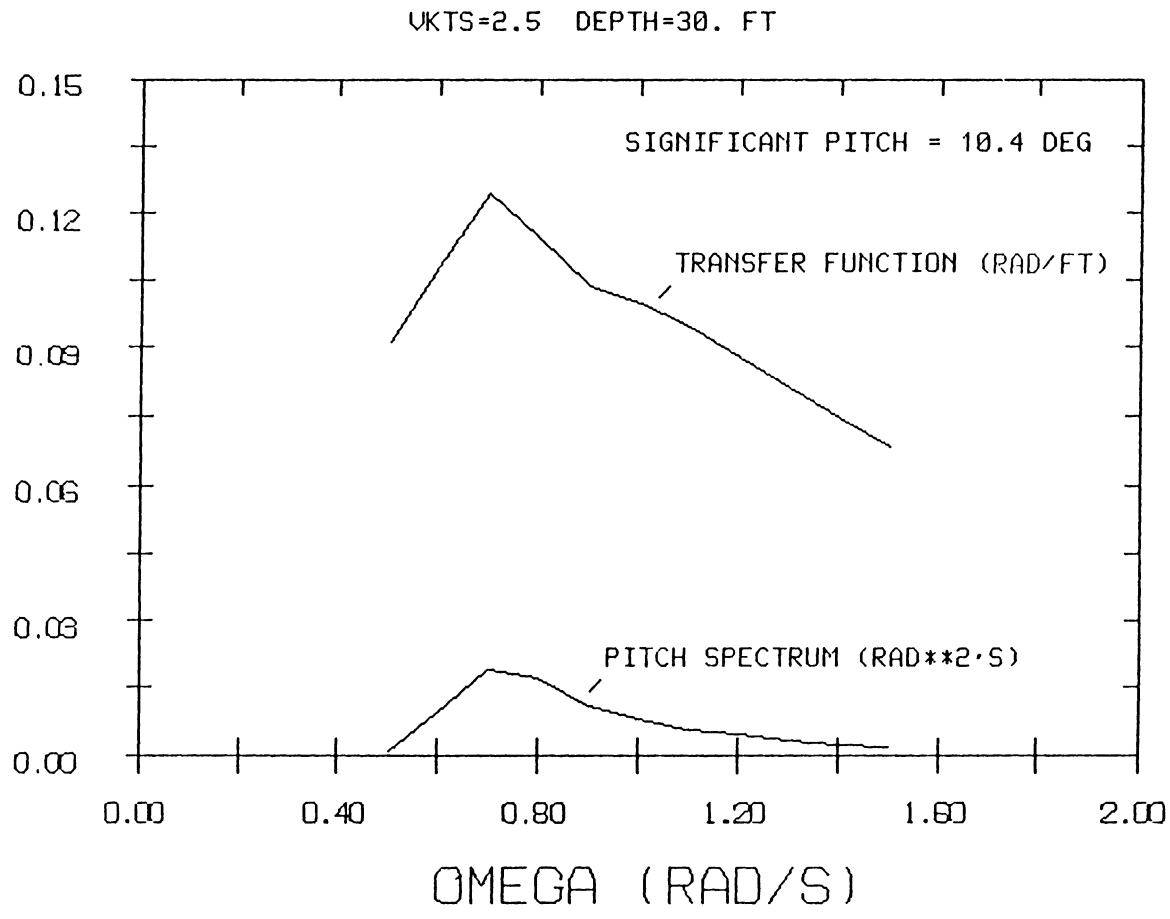

FIGURE 21. TRANSFER FUNCTION AND SPECTRUM (PITCH) FOR VEHICLE AT 2.5 KT AND 30 FT DEPTH

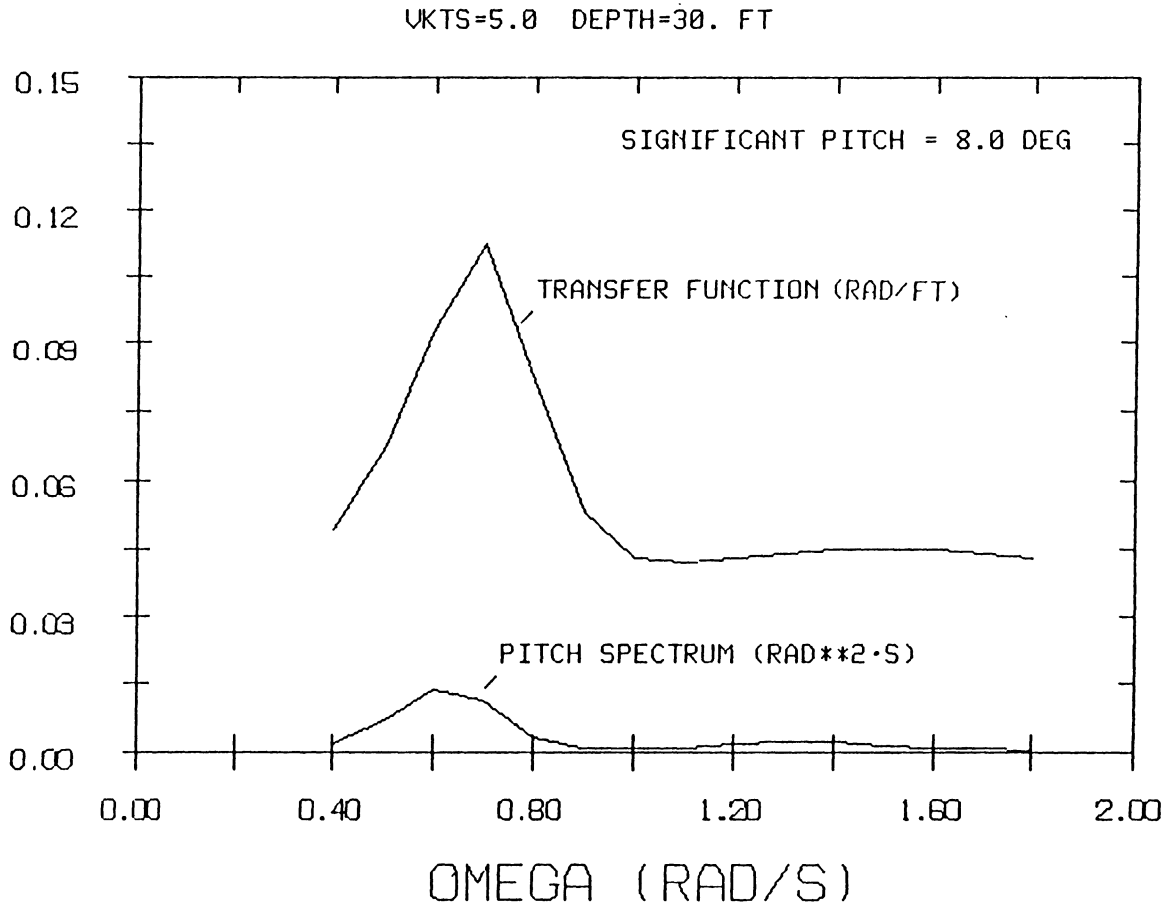

FIGURE 22. TRANSFER FUNCTION AND SPECTRUM (PITCH) FOR VEHICLE AT 5.0 KT AND 30 FT DEPTH

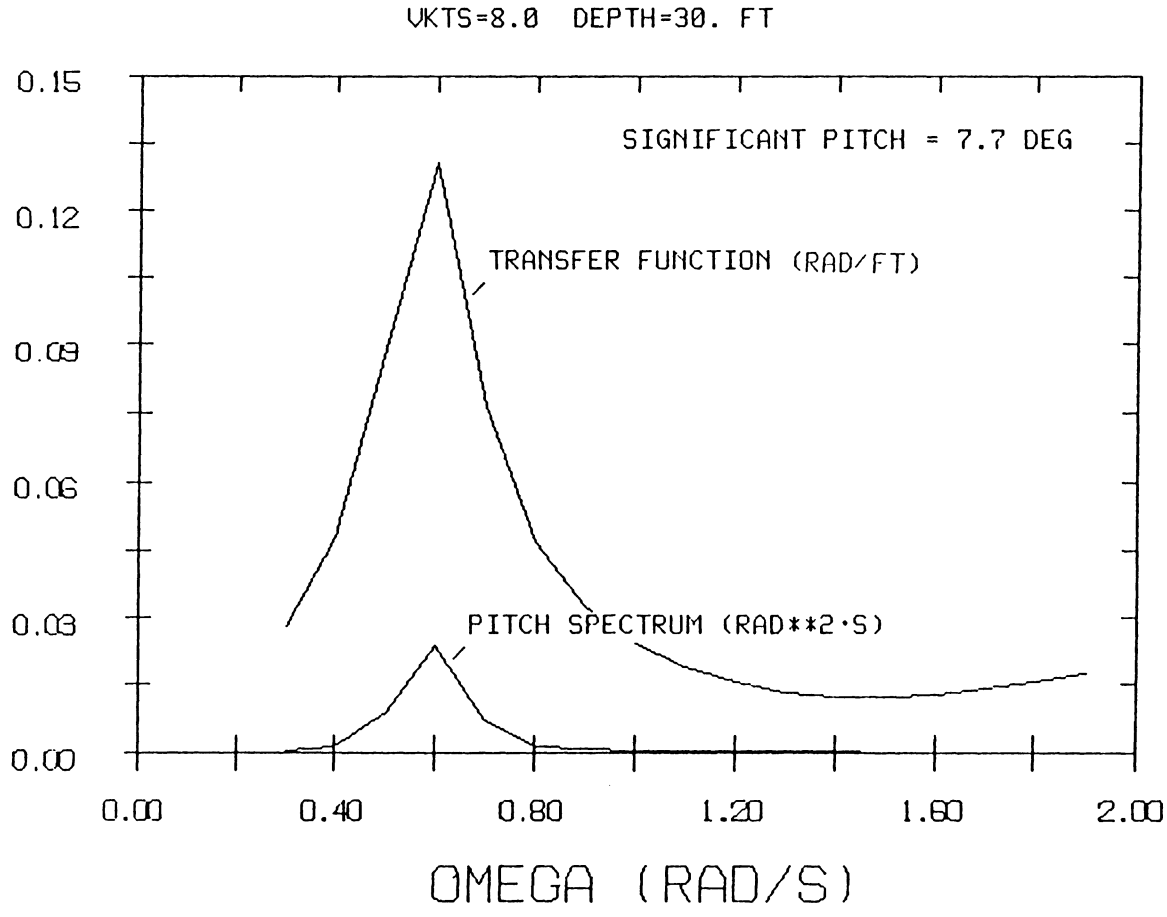

FIGURE 23. TRANSFER FUNCTION AND SPECTRUM (PITCH) FOR VEHICLE AT 8.0 KT AND 30 FT DEPTH

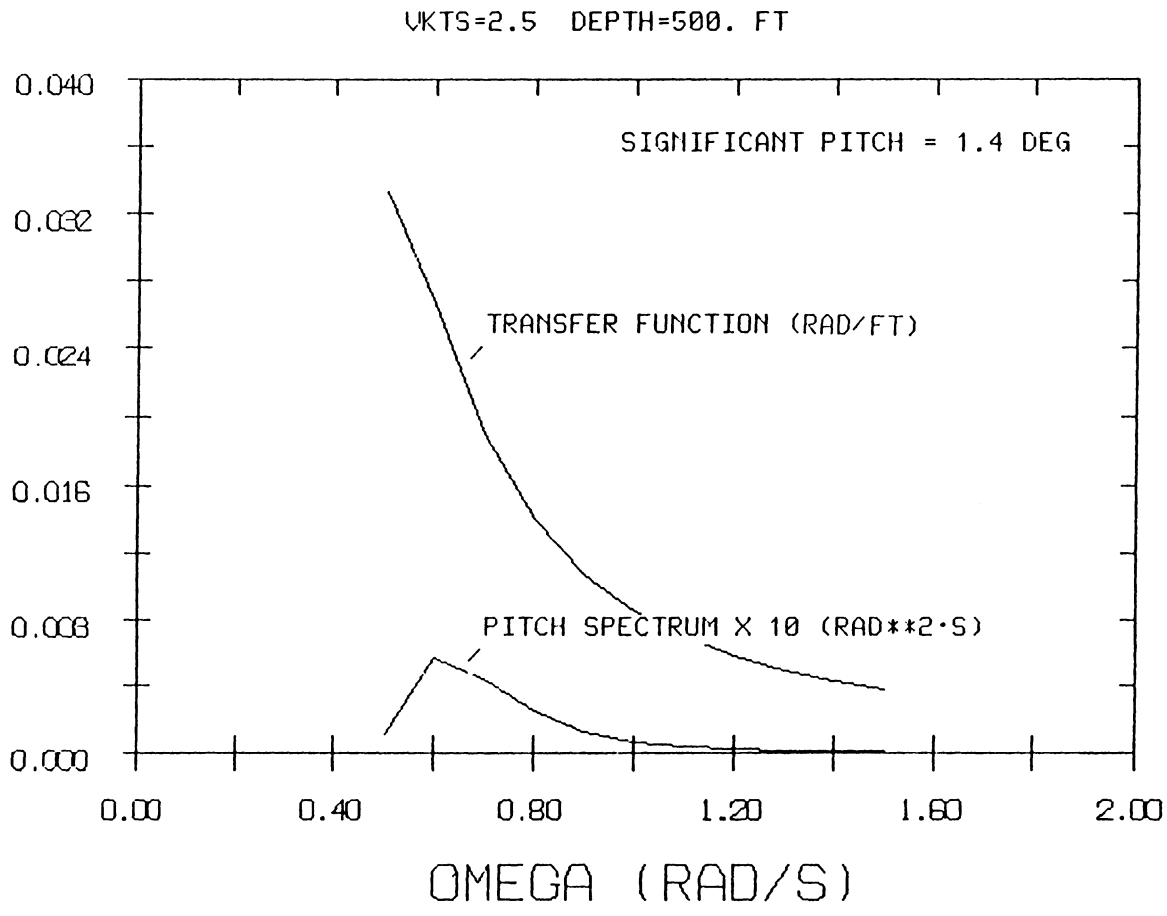

FIGURE 24. TRANSFER FUNCTION AND SPECTRUM (PITCH) FOR VEHICLE AT 2.5 KT AND 500 FT DEPTH

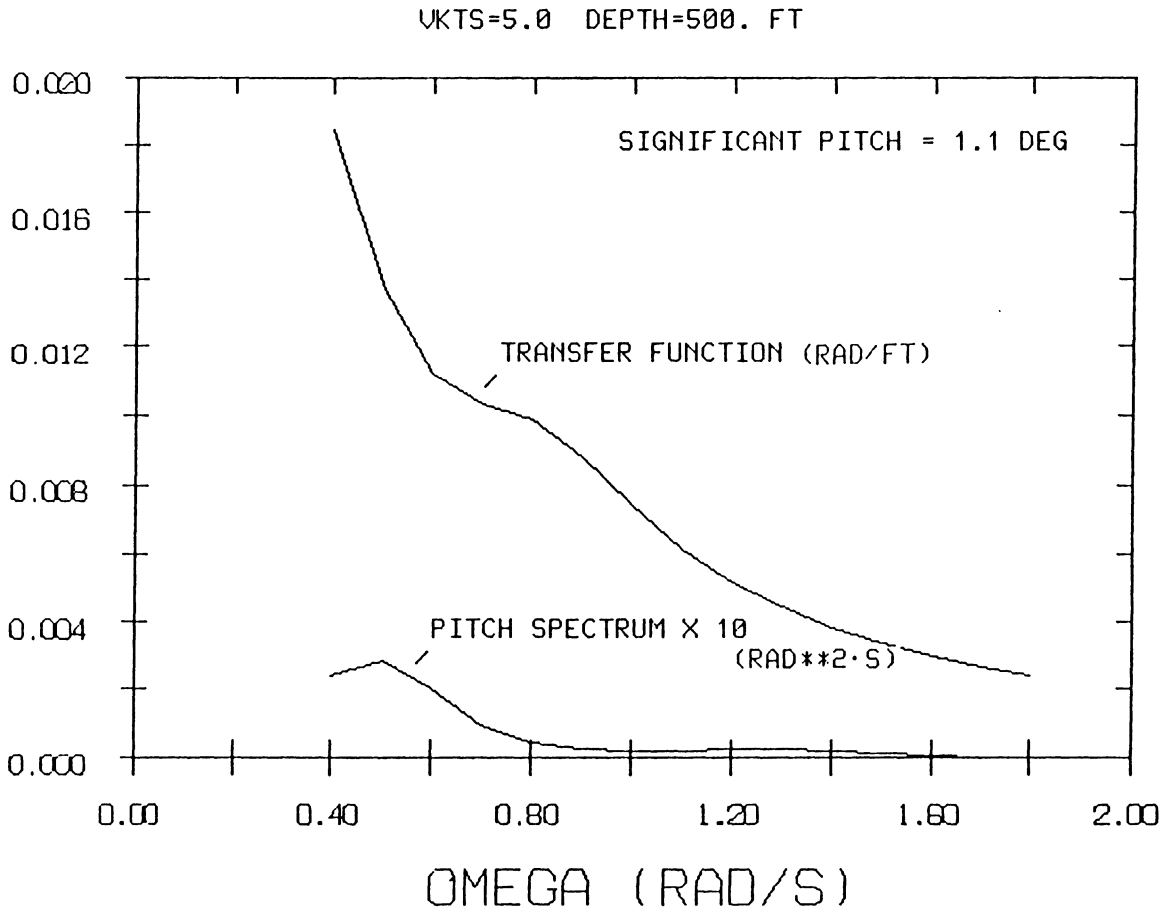

FIGURE 25. TRANSFER FUNCTION AND SPECTRUM (PITCH) FOR VEHICLE AT 5.0 KT AND 500 FT DEPTH

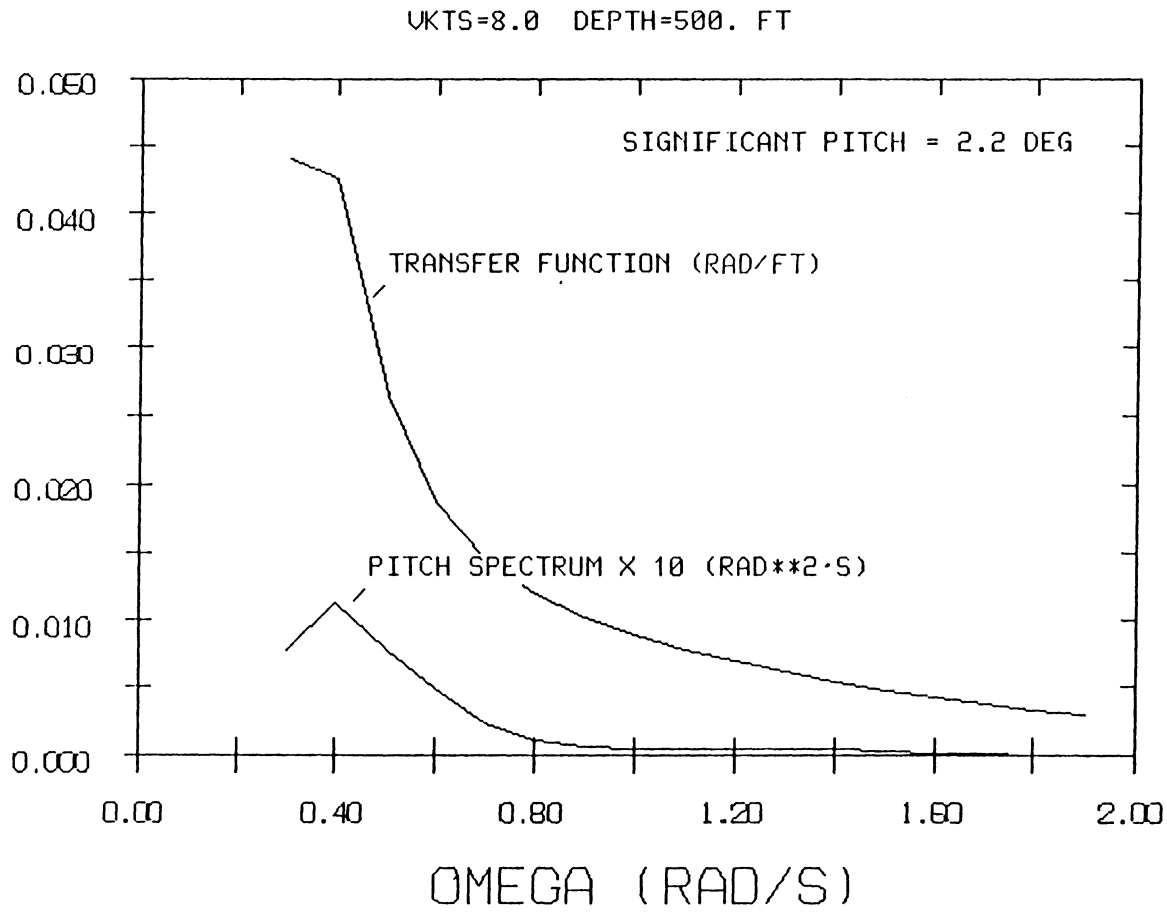

FIGURE 26. TRANSFER FUNCTION AND SPECTRUM (PITCH) FOR VEHICLE AT 8.0 KT AND 500 FT DEPTH

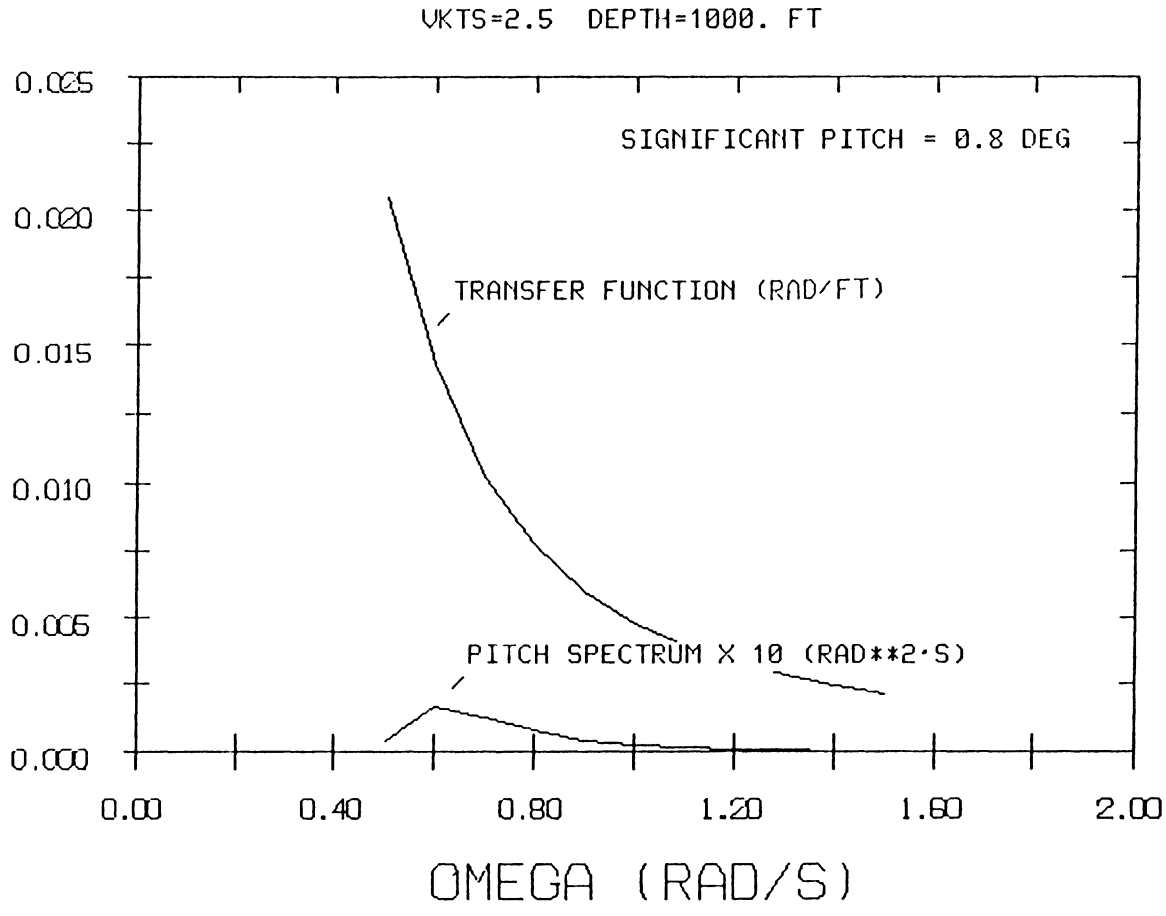

FIGURE 27. TRANSFER FUNCTION AND SPECTRUM (PITCH) FOR VEHICLE AT 2.5 KT AND 1000 FT DEPTH

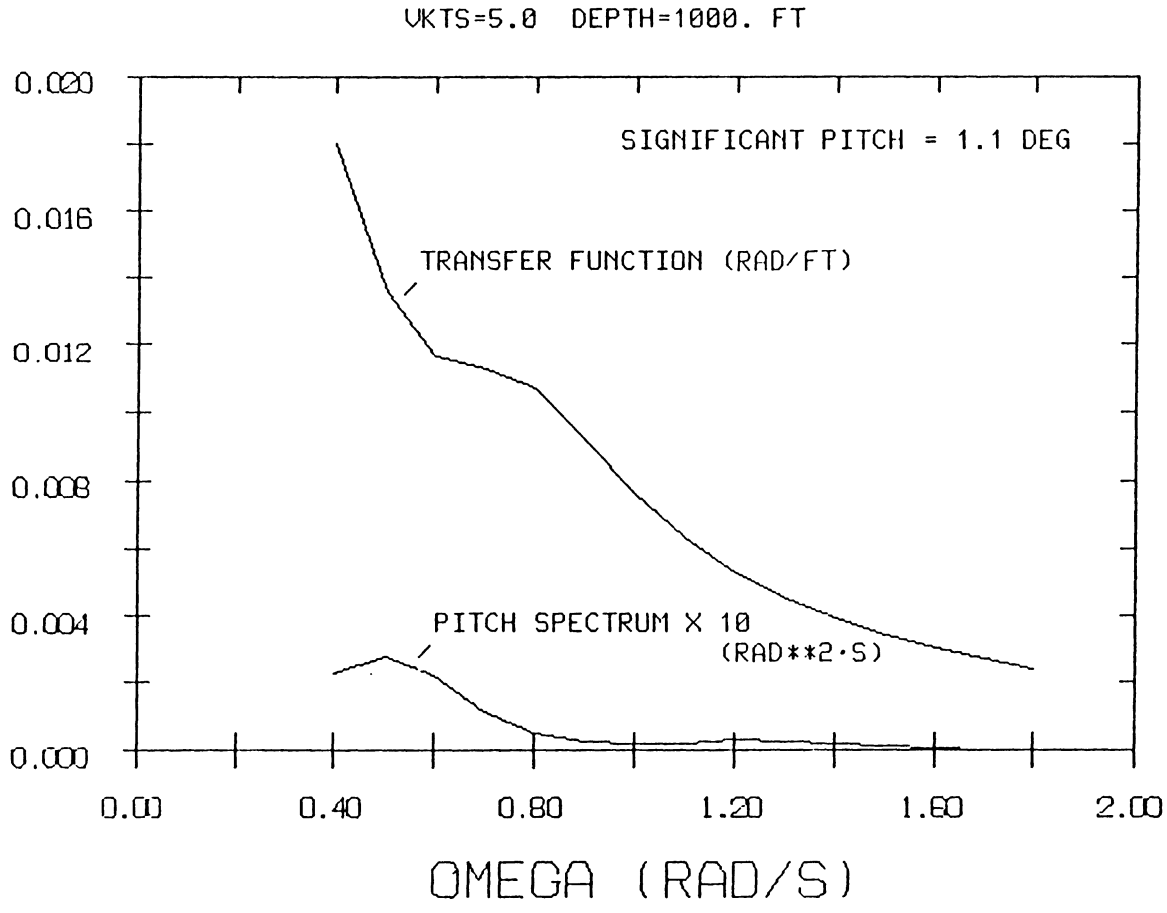

FIGURE 28. TRANSFER FUNCTION AND SPECTRUM (PITCH) FOR VEHICLE AT 5.0 KT AND 1000 FT DEPTH

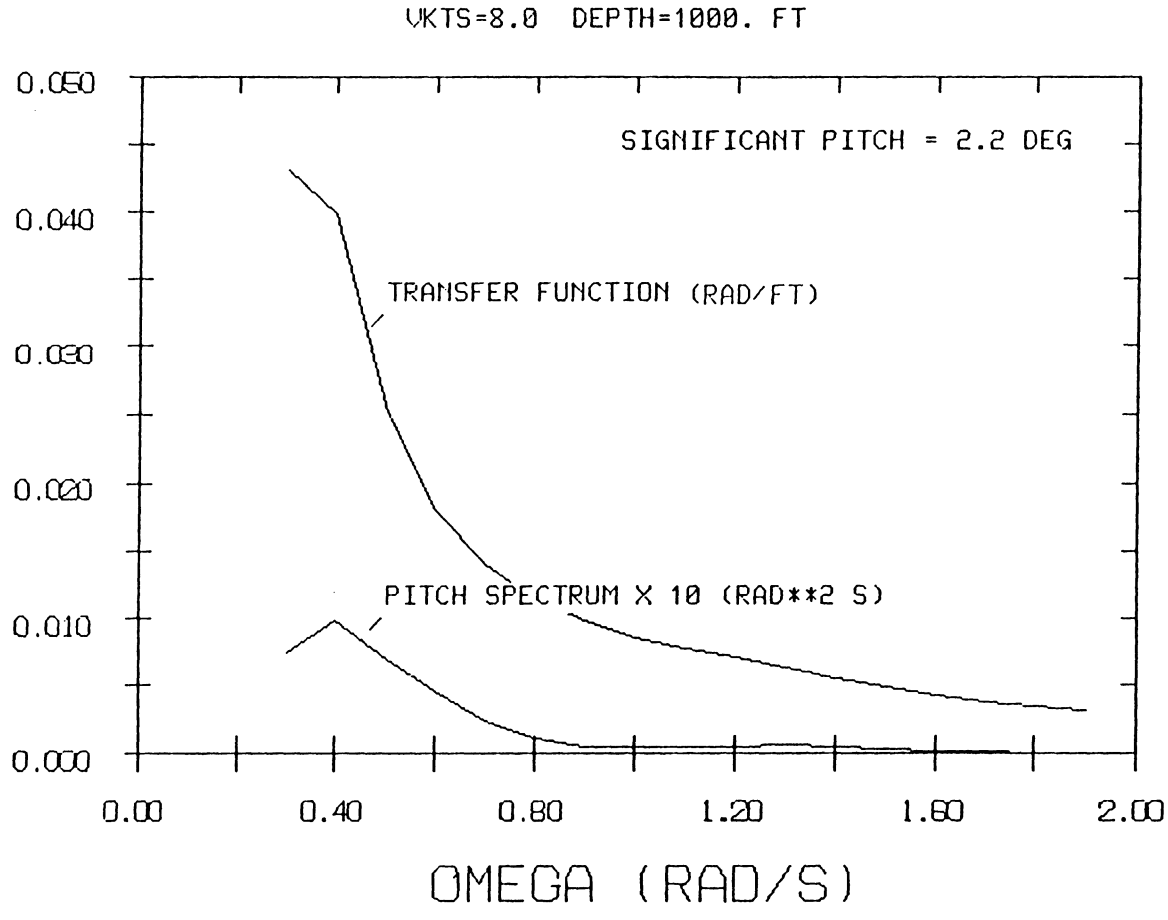

FIGURE 29. TRANSFER FUNCTION AND SPECTRUM (PITCH) FOR VEHICLE A AT 8.0 KT AND 1000 FT DEPTH

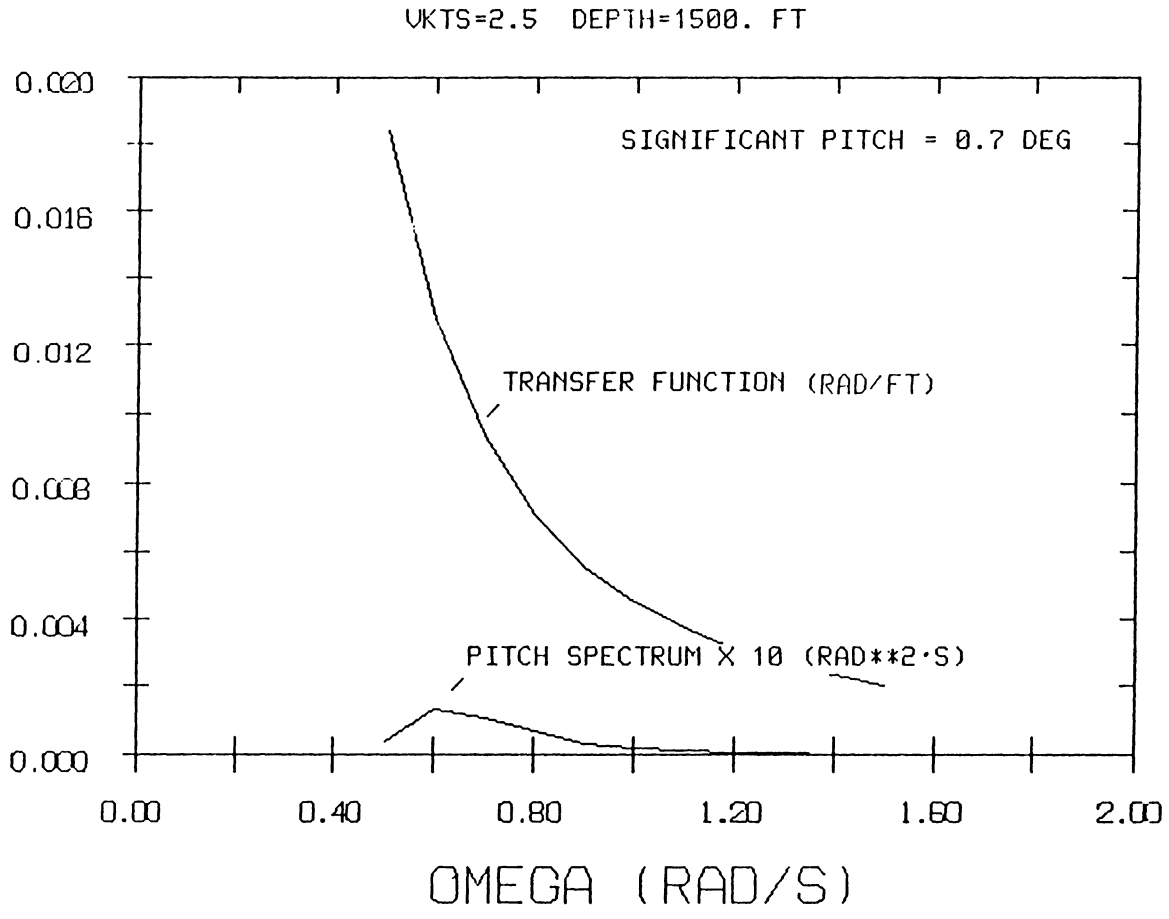

FIGURE 30. TRANSFER FUNCTION AND SPECTRUM (PITCH) FOR VEHICLE A AT 2.5 KT AND 1500 FT DEPTH

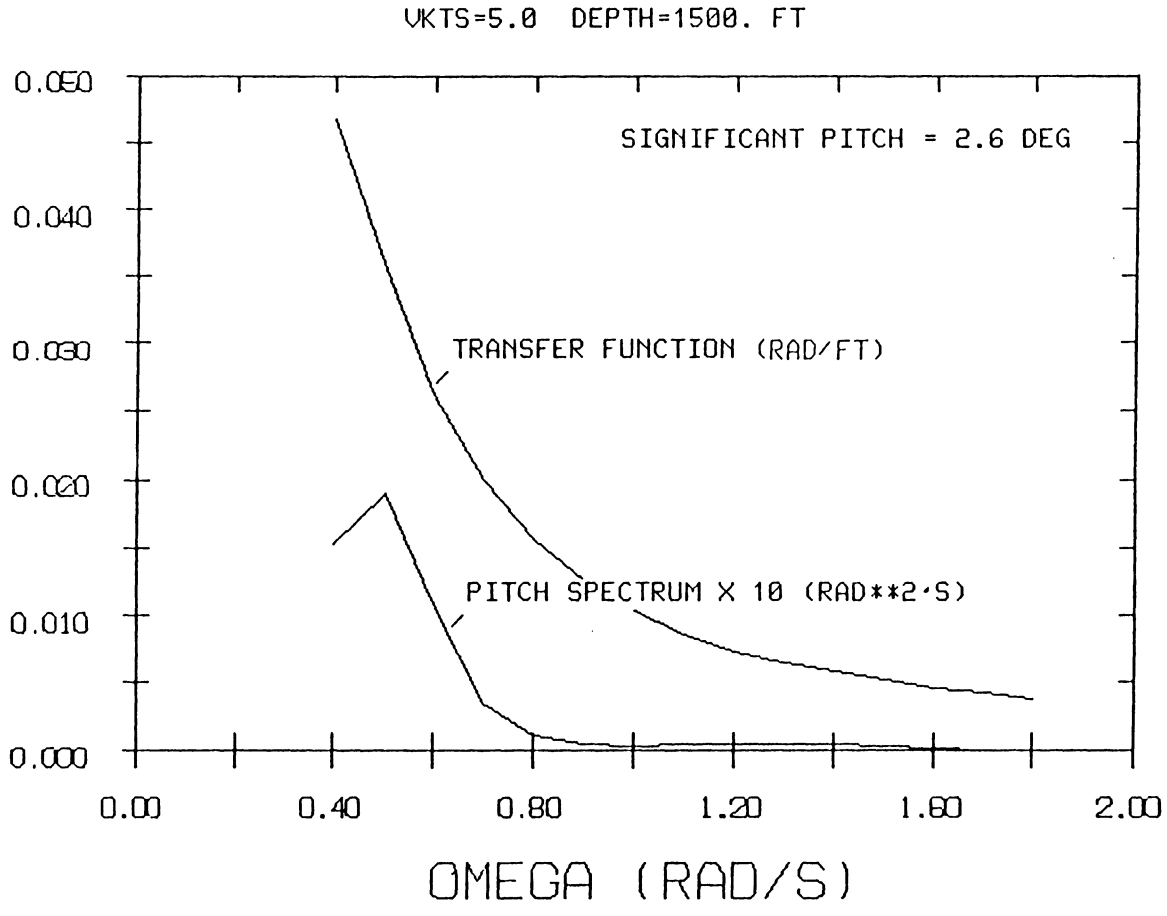

FIGURE 31. TRANSFER FUNCTION AND SPECTRUM (PITCH) FOR VEHICLE A AT 5.0 KT AND 1500 FT DEPTH

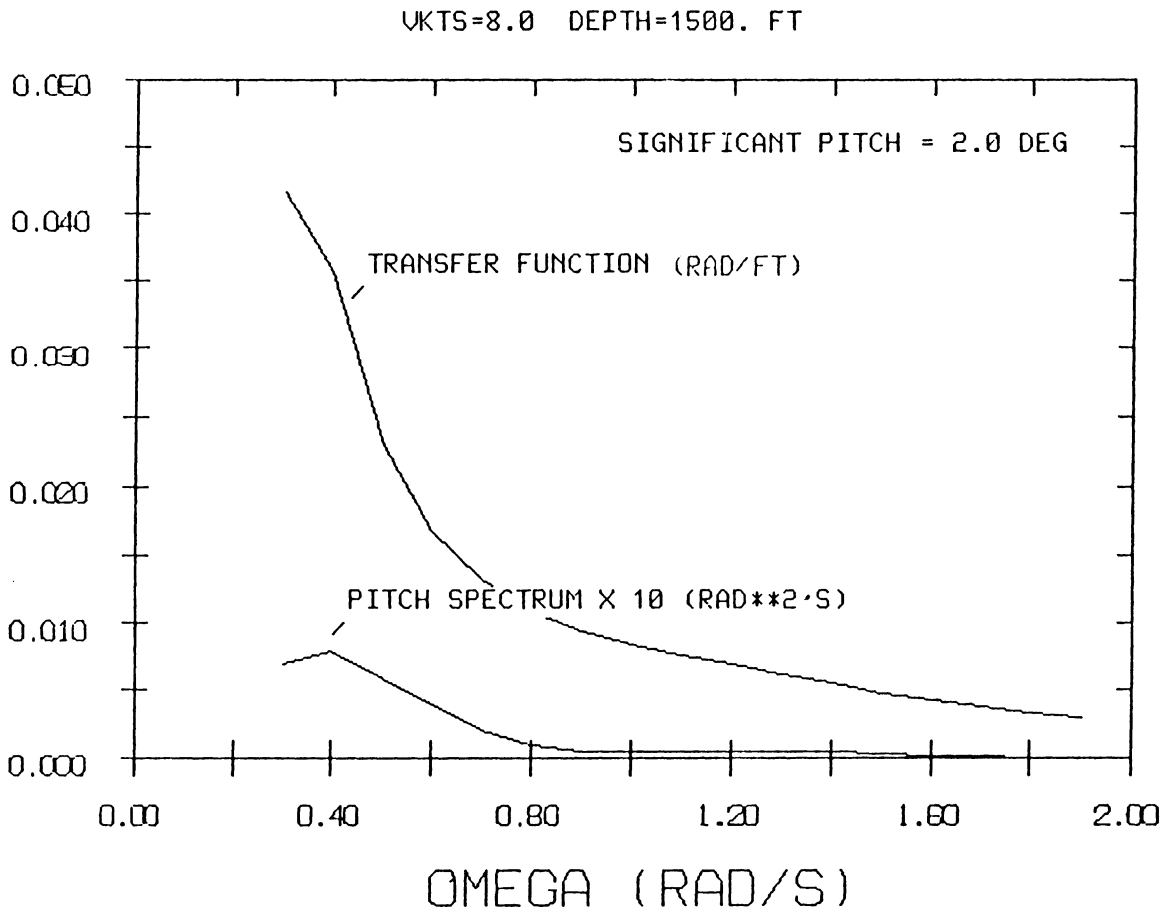

FIGURE 32. TRANSFER FUNCTION AND SPECTRUM (PITCH) FOR VEHICLE A AT 8.0 KT AND 1500 FT DEPTH

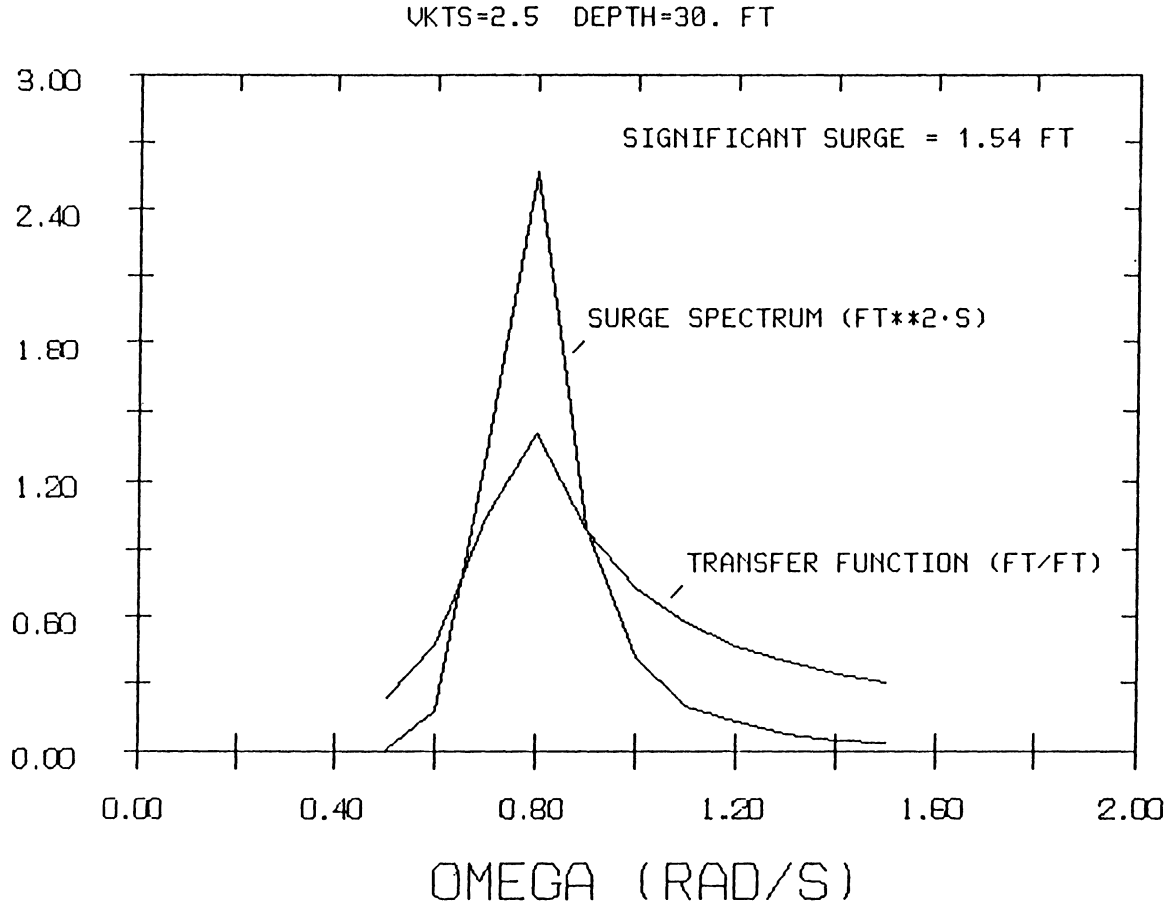

FIGURE 33. TRANSFER FUNCTION AND SPECTRUM (SURGE) FOR VEHICLE A AT 2.5 KT AND 30 FT DEPTH

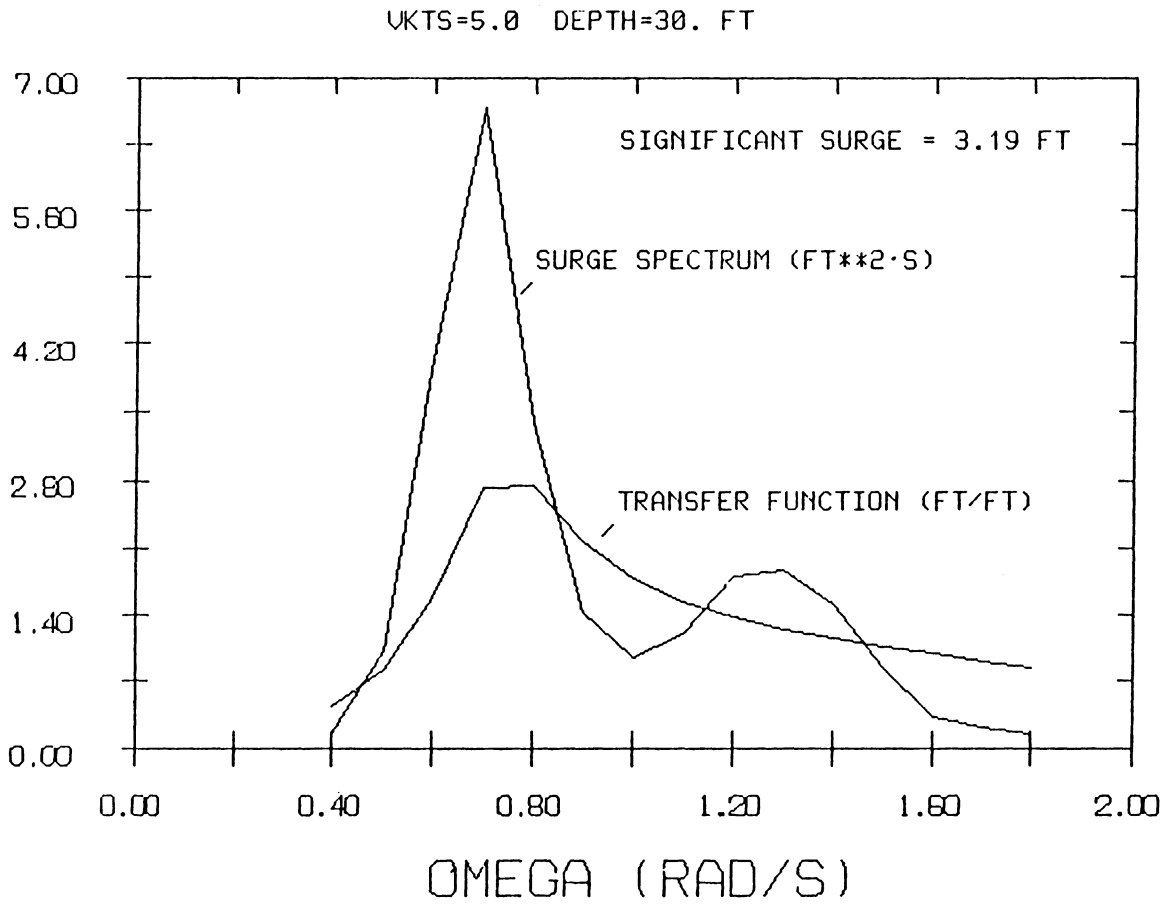

FIGURE 34. TRANSFER FUNCTION AND SPECTRUM (SURGE) FOR VEHICLE A AT 5.0 KT AND 30 FT DEPTH

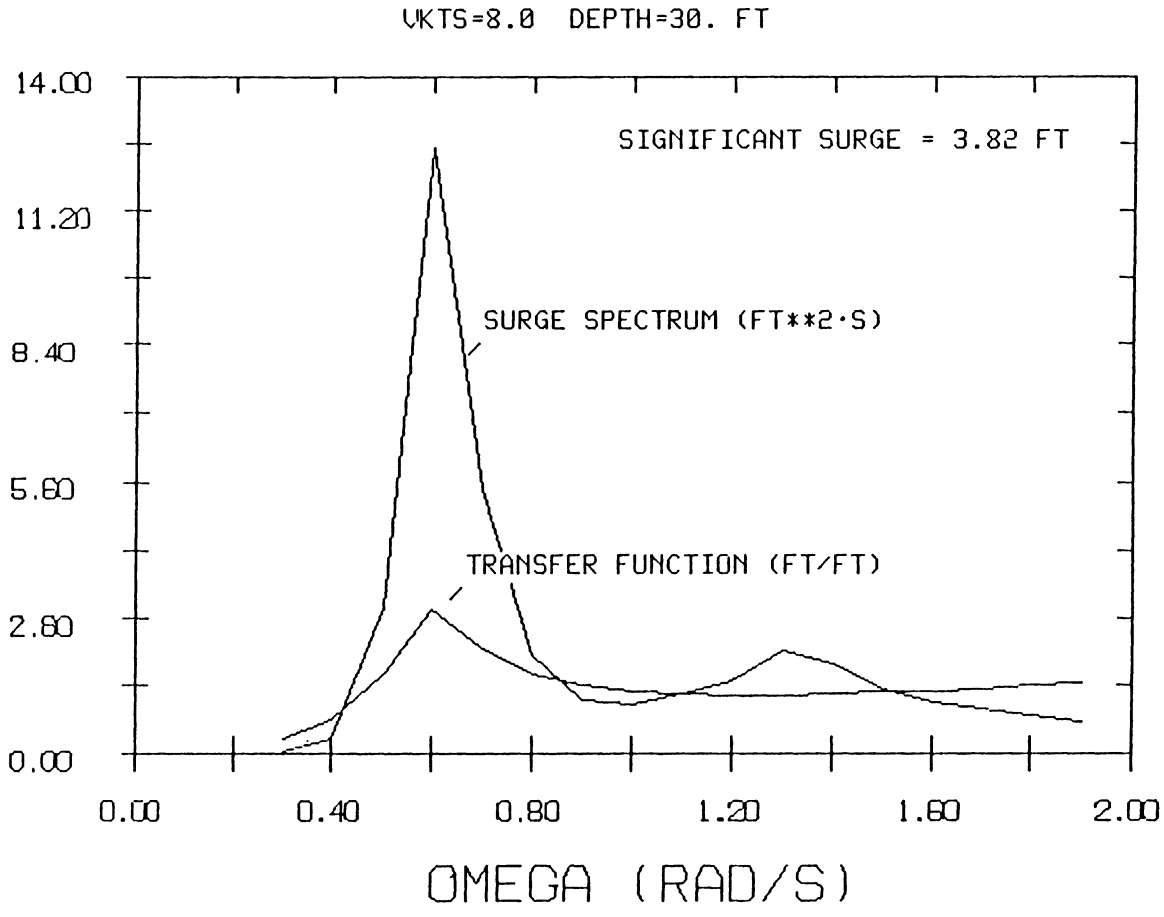

FIGURE 35. TRANSFER FUNCTION AND SPECTRUM (SURGE) FOR VEHICLE A AT 8.0 KT AND 30 FT DEPTH

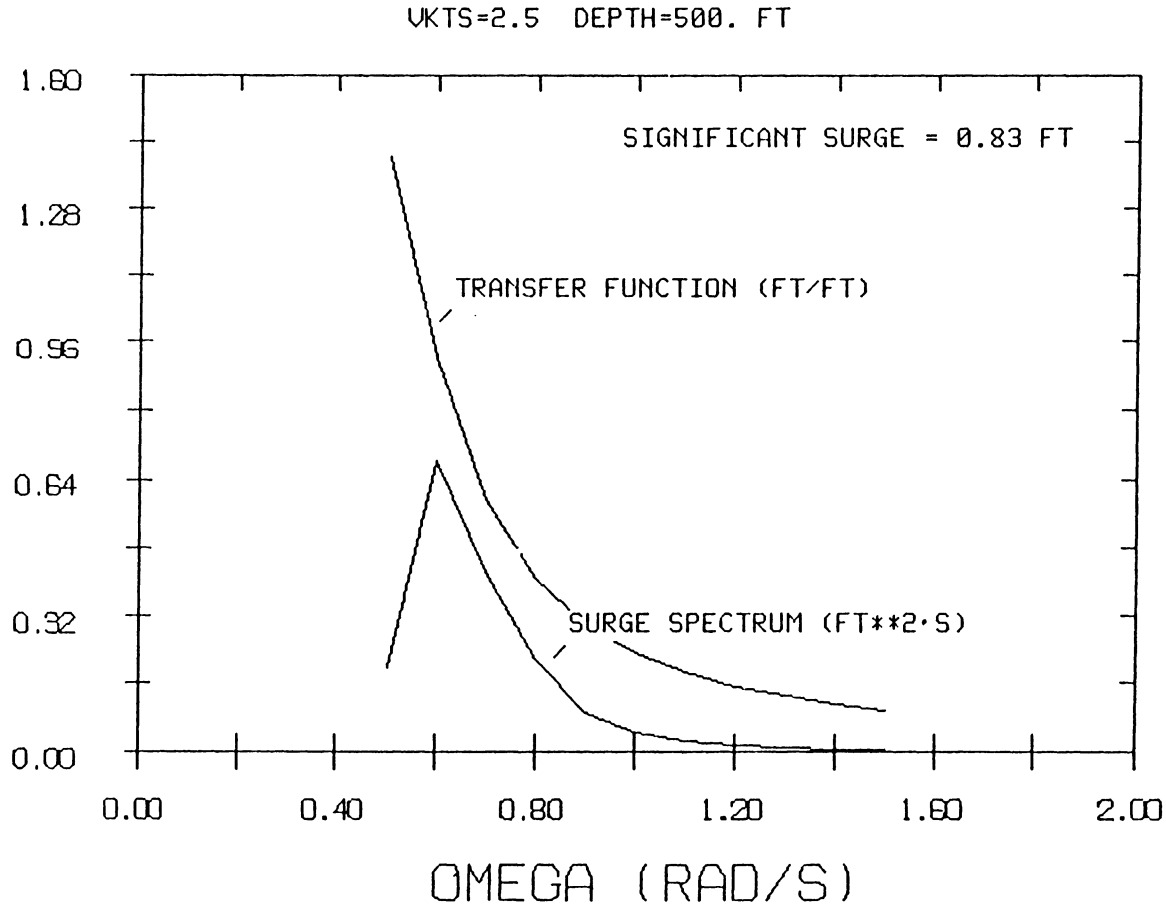

FIGURE 36. TRANSFER FUNCTION AND SPECTRUM (SURGE) FOR VEHICLE A AT 2.5 KT AND 500 FT DEPTH

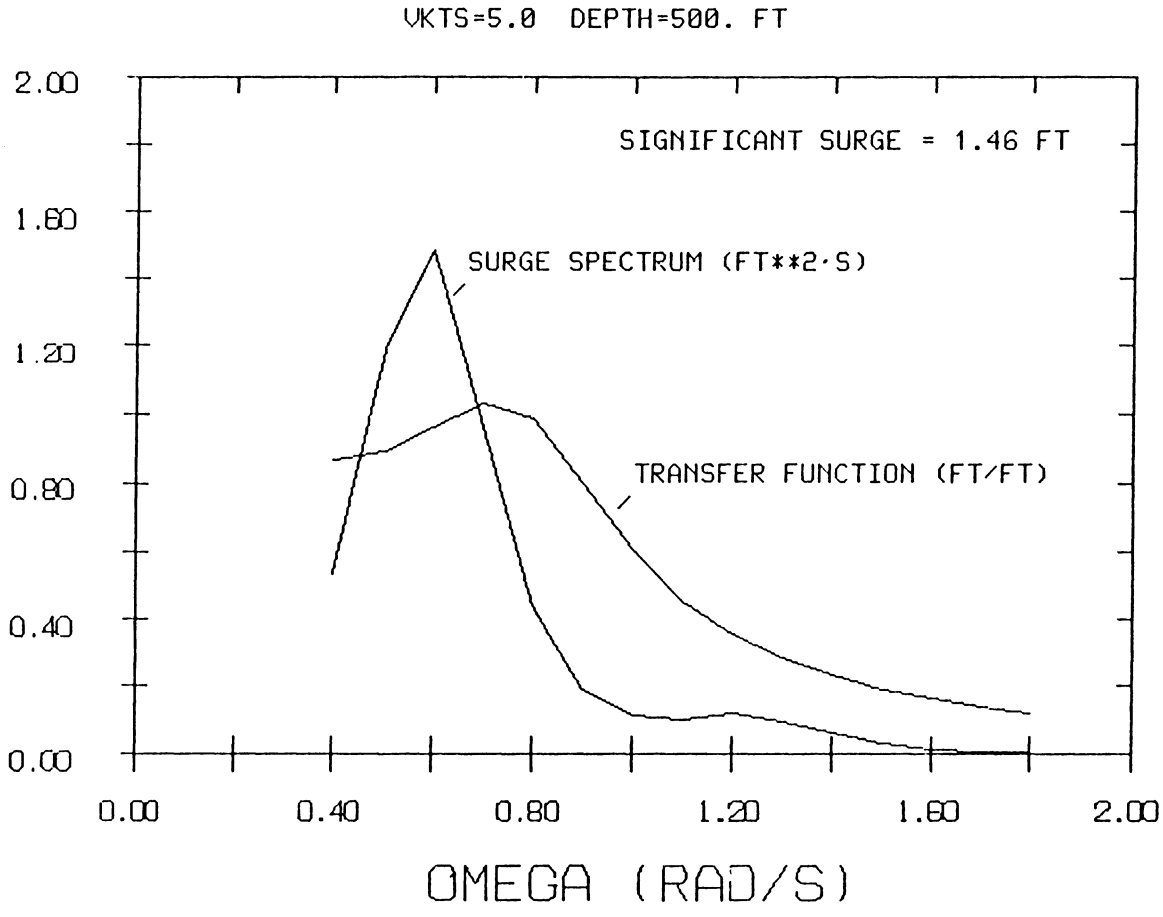

FIGURE 37. TRANSFER FUNCTION AND SPECTRUM (SURGE) FOR VEHICLE A AT 5.0 KT AND 500 FT DEPTH

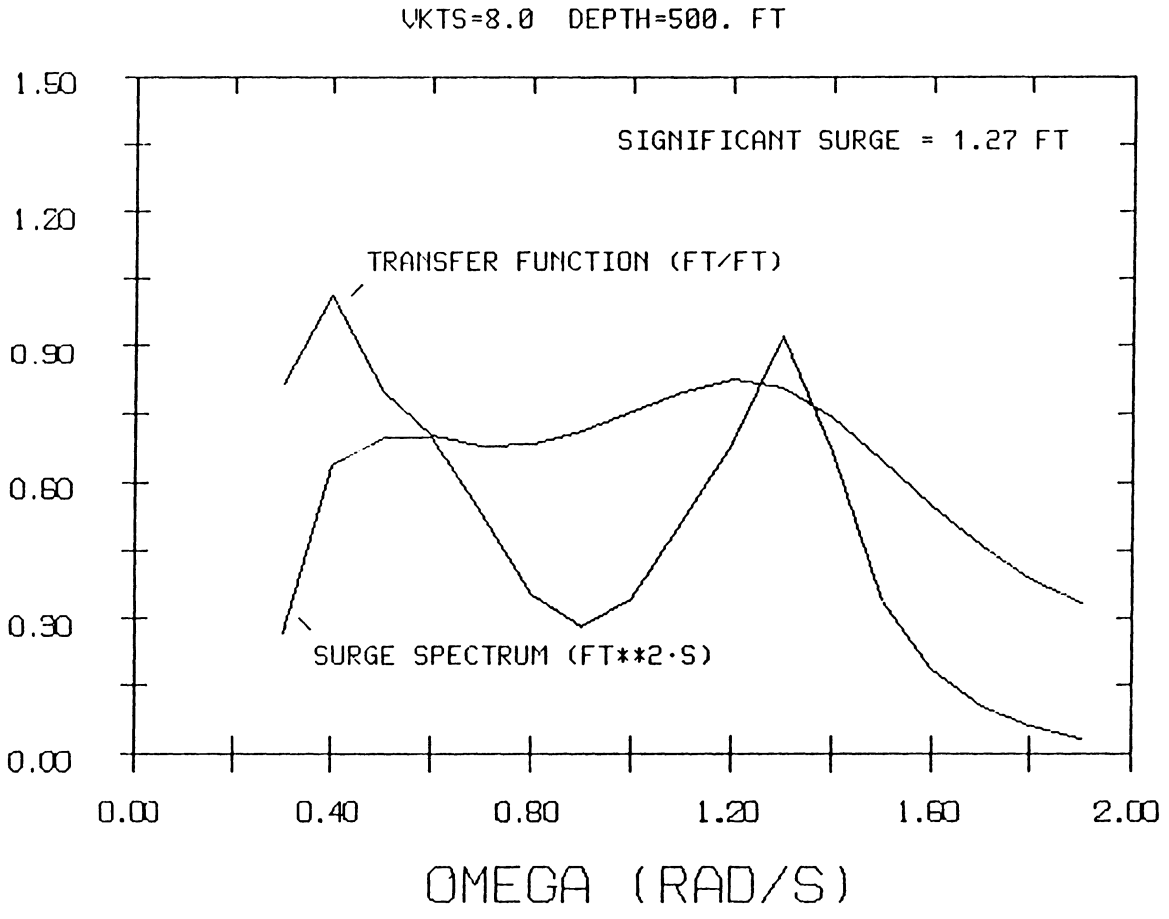

FIGURE 38. TRANSFER FUNCTION AND SPECTRUM (SURGE) FOR VEHICLE A AT 8.0 KT AND 500 FT DEPTH

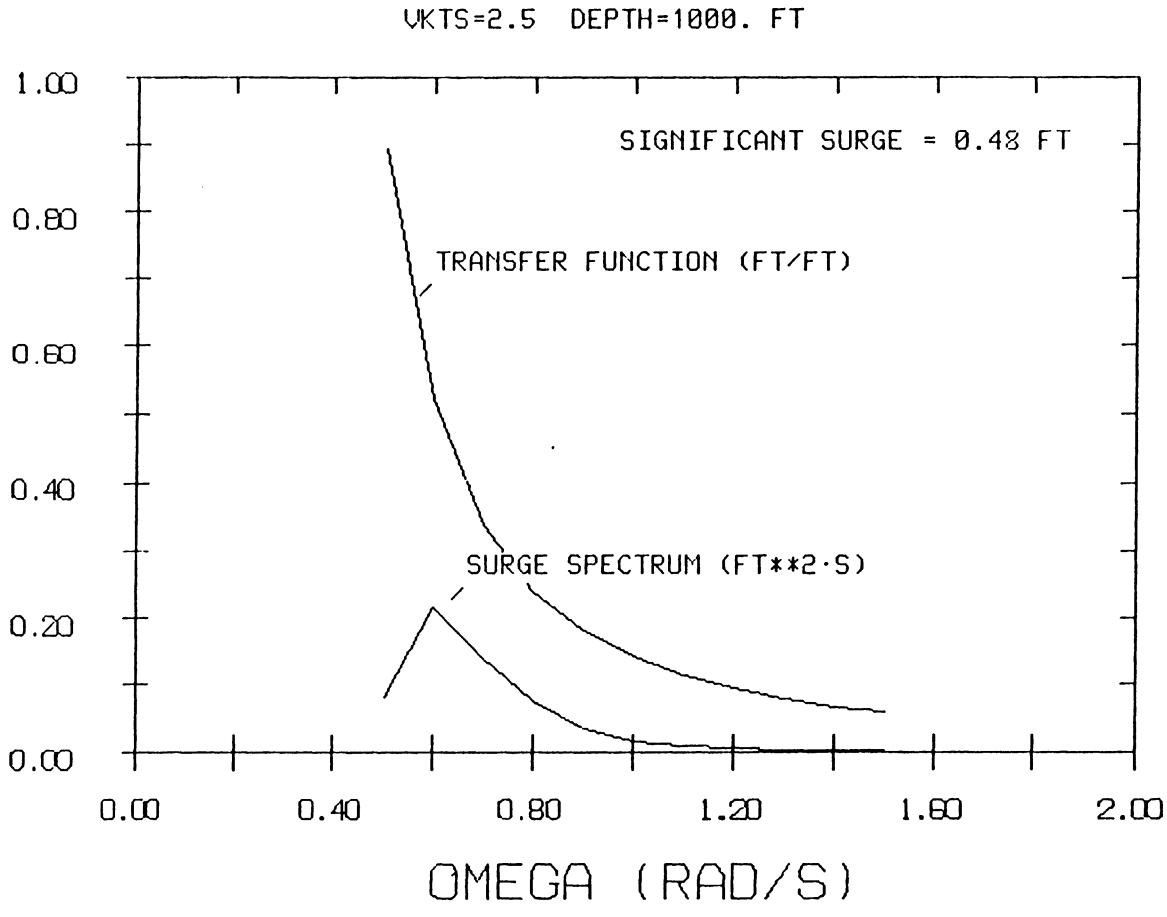

FIGURE 39. TRANSFER FUNCTION AND SPECTRUM (SURGE) FOR VEHICLE A AT 2.5 KT AND 1000 FT DEPTH

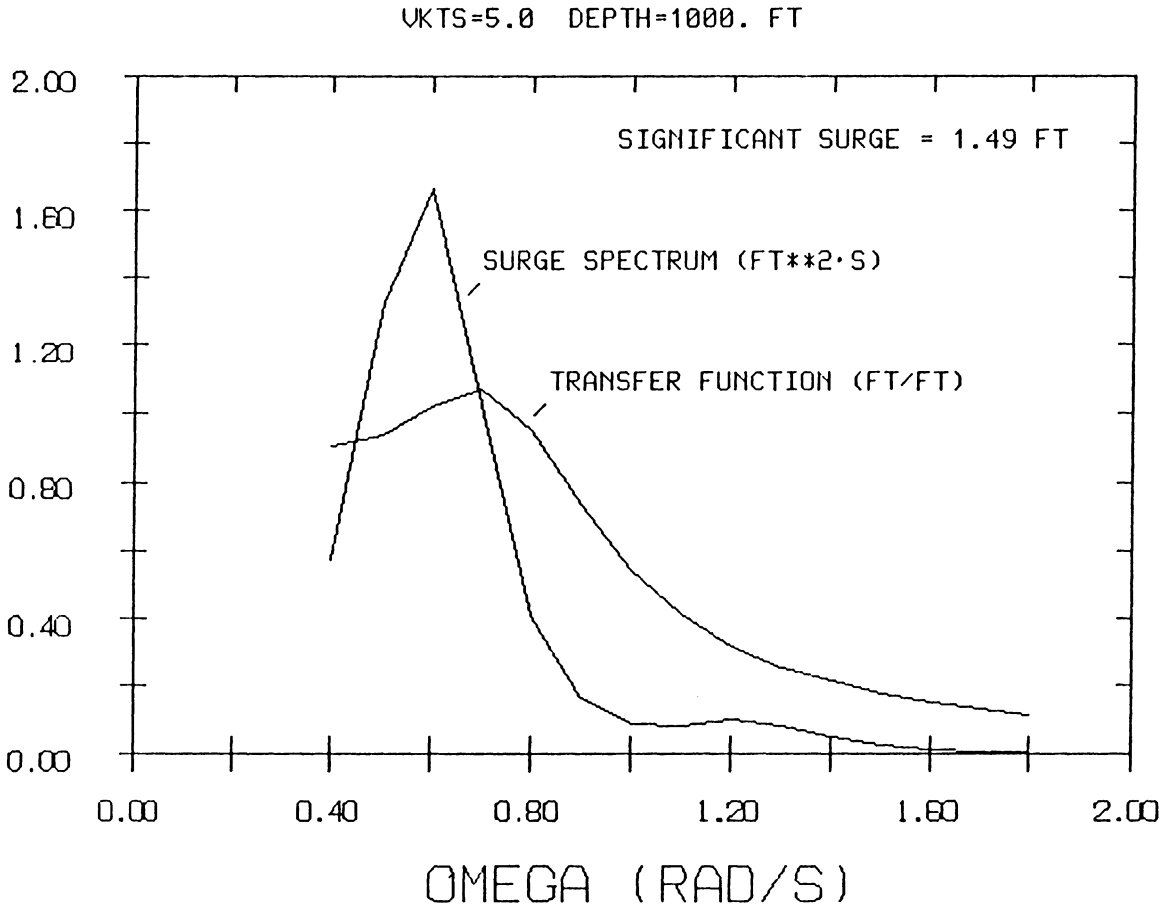

FIGURE 40. TRANSFER FUNCTION AND SPECTRUM (SURGE) FOR VEHICLE A AT 5.0 KT AND 1000 FT DEPTH

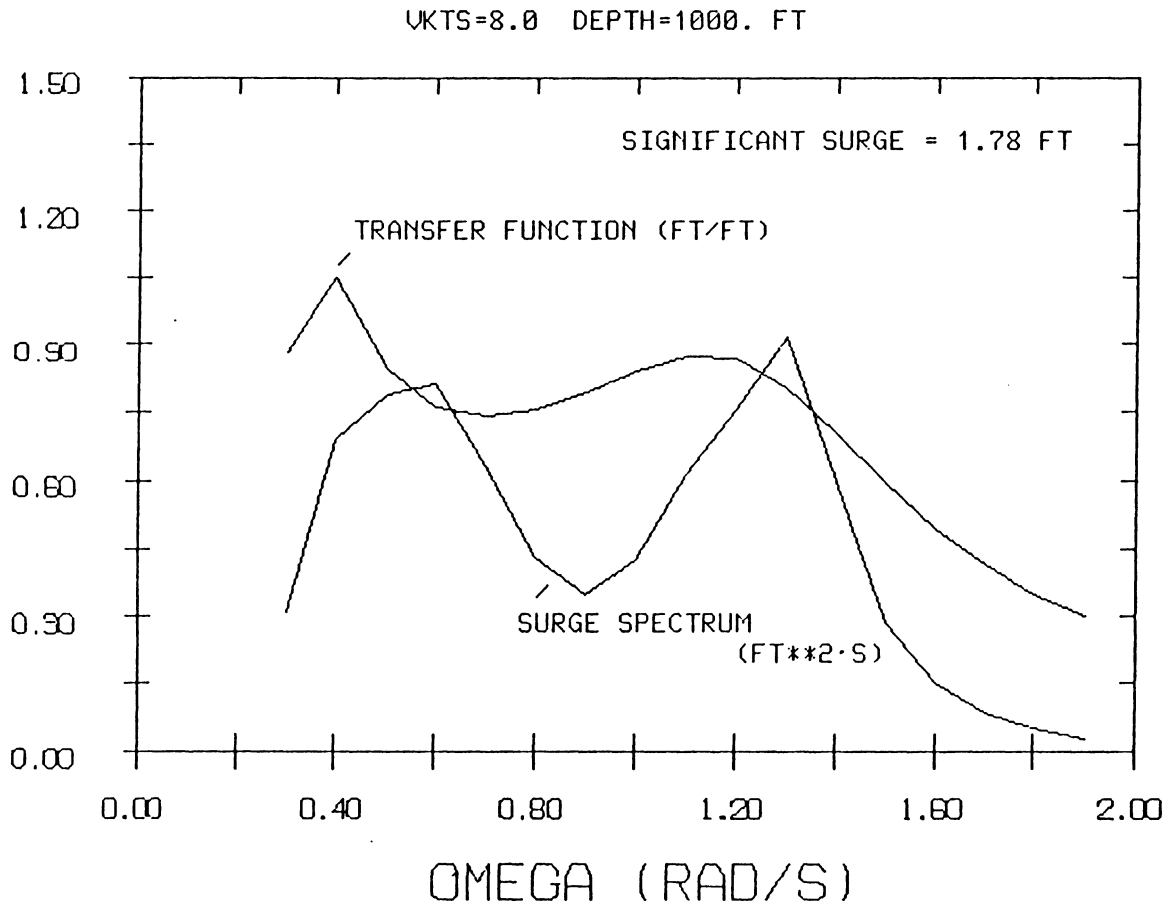

FIGURE 41. TRANSFER FUNCTION AND SPECTRUM (SURGE) FOR VEHICLE A AT 8.0 KT AND 1000 FT DEPTH

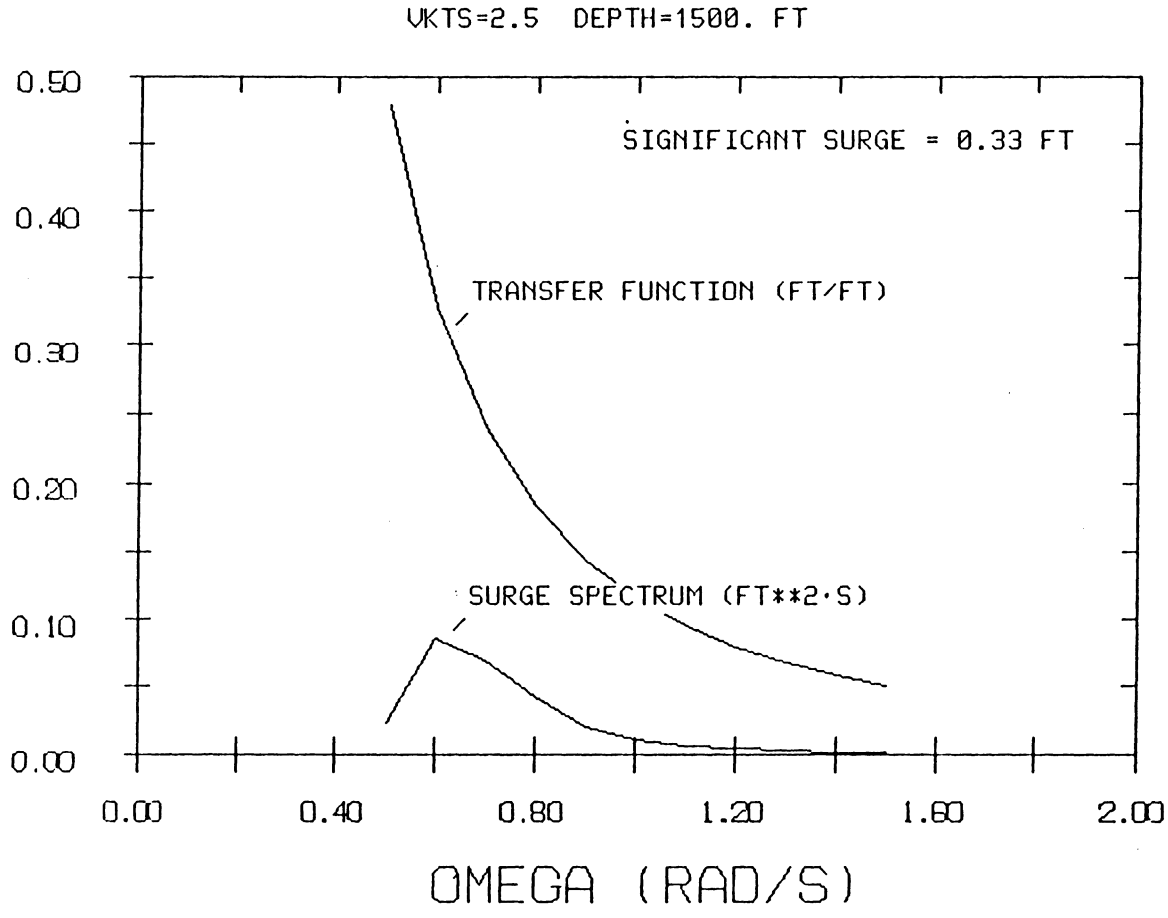

FIGURE 42. TRANSFER FUNCTION AND SPECTRUM (SURGE) FOR VEHICLE A AT 2.5 KT AND 1500 FT DEPTH

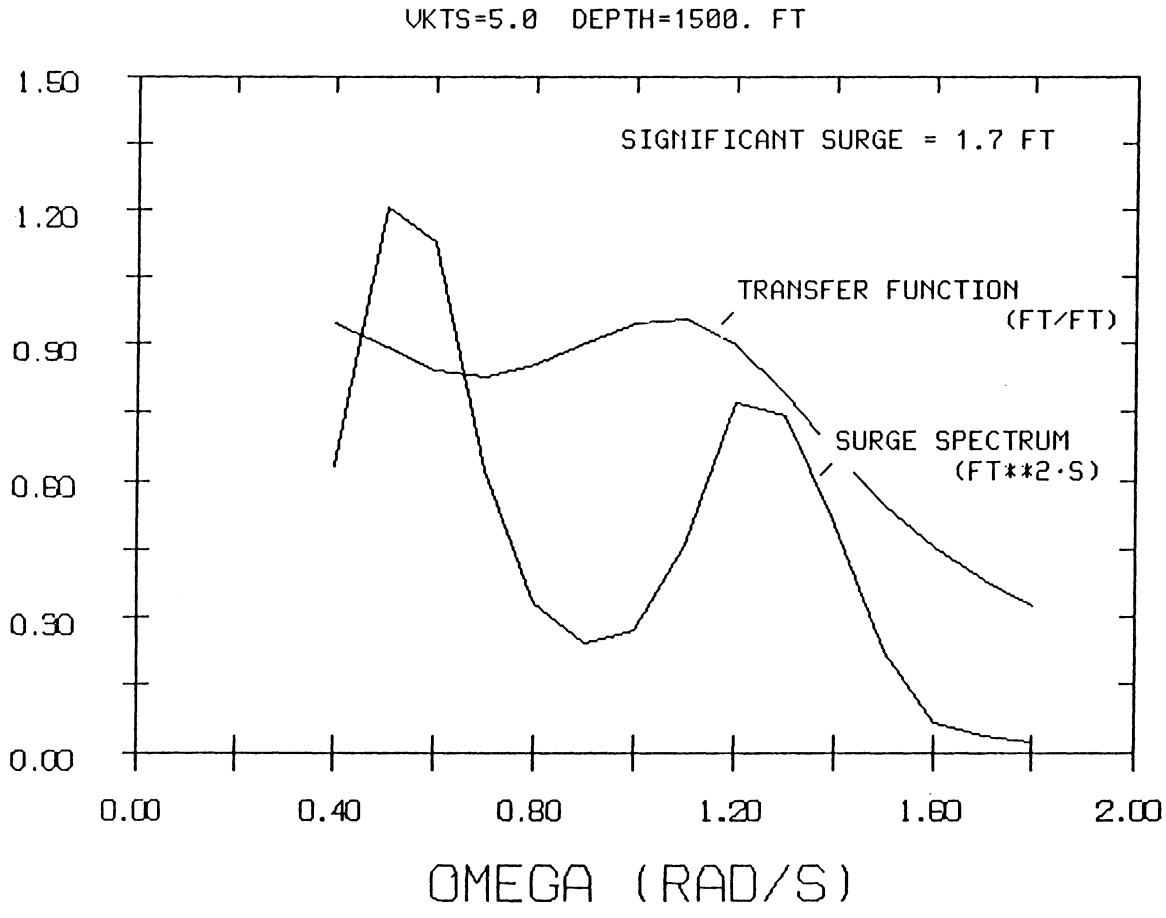

FIGURE 43. TRANSFER FUNCTION AND SPECTRUM (SURGE) FOR VEHICLE A AT 5.0 KT AND 1500 FT DEPTH

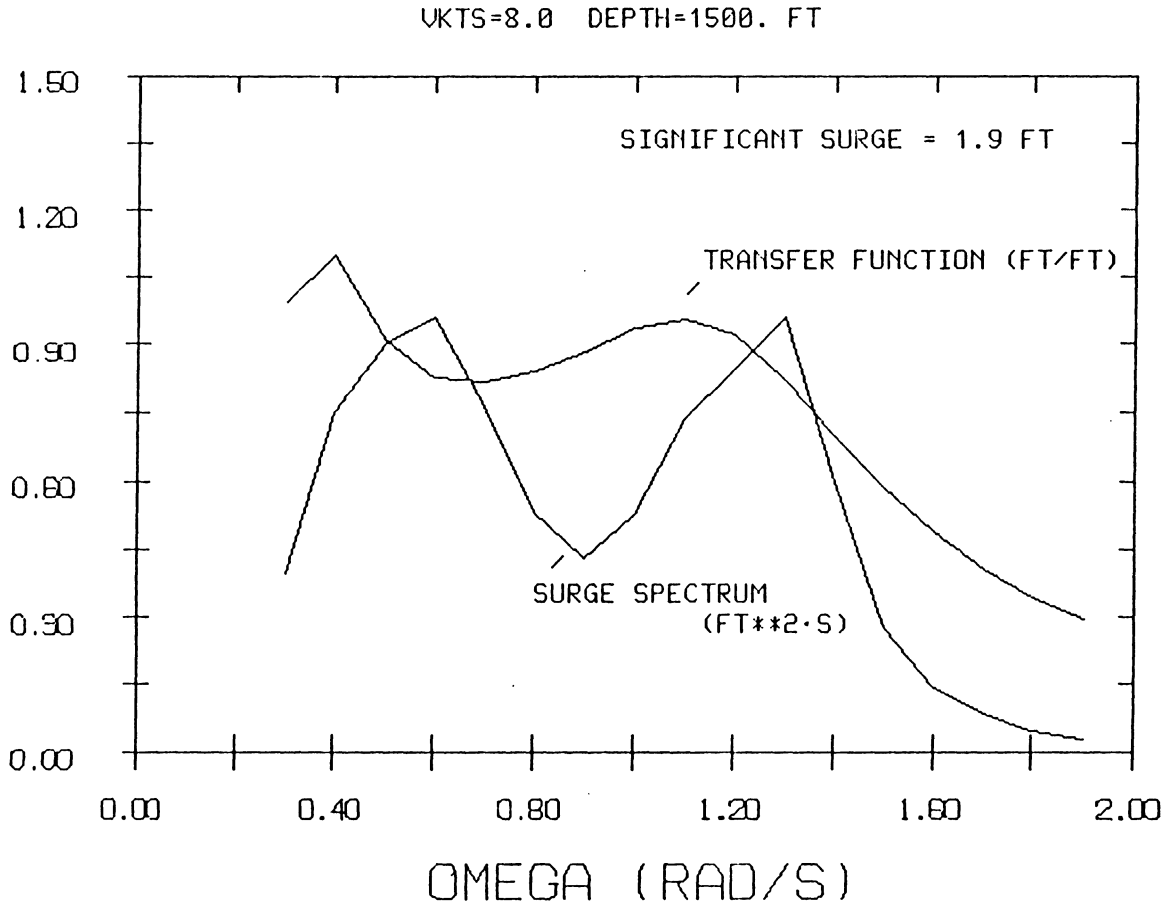

FIGURE 44. TRANSFER FUNCTION AND SPECTRUM (SURGE) FOR VEHICLE A AT 8.0 KT AND 1500 FT DEPTH

The vita has been removed
from the scanned document